Inst
Hydrology

1991/069

ARCHIVE:

PLEASE DO NOT DESTROY

MINISTRY OF AGRICULTURE FISHERIES AND FOOD

PROJECT AA2

PHYSICALLY-BASED DISTRIBUTED
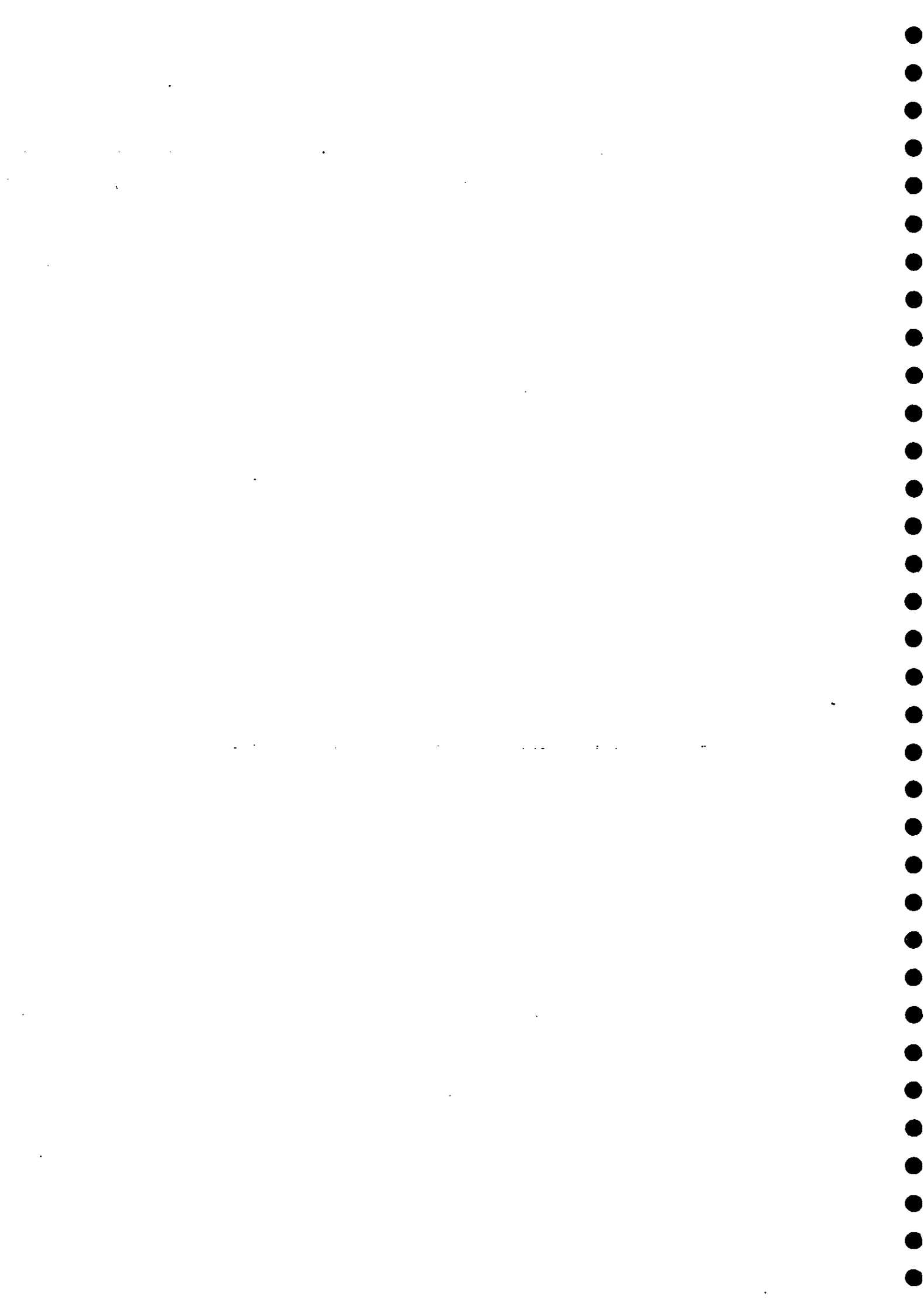CATCHMENT MODELS

PORTFOLIO OF PUBLISHED
RESEARCH RESULTS   1991

Ann Calver

November 1991

CONTENTS

PROJECT: AA2
                               PHYSICALLY-BASED DISTRIBUTED
                               CATCHMENT MODELS

CONTRACTOR: Institute of Hydrology

PROJECT STAFF: Dr A Calver, Mr D Lewis,
                               Ms L Buckle (until July 1991),
                               Ms N Hasnip (from July 1991)

MAFF RESPONSIBLE OFFICER: Mr R Buckingham

DATE: 15 October 1991

OBJECTIVE:

The prediction of hydrological responses by means of physically-
based distributed catchment models for research and engineering
purposes.

REVIEW OF PROGRESS APRIL-OCTOBER 1991:

The research programme has continued to pursue a number of
complementary lines of investigation into physically-based
rainfall-runoff modelling, highlights of which are outlined
below. These include:-

1.   Concise nomographs for peak flow prediction
2.   Definition of guidelines for model initial conditions
3.   Error surface determinations
4.   Exploratory design of partially-distributed models.

1.   The IH Distributed Model (IHDM) is the main model developed
in this programme, solving numerically interlinked surface and
subsurface flow equations. Generalised procedures for the
concise and non-dimensional representation of peak discharges and
times-to-peak in relation to physical factors have been
established, and nomographs have been produced for two specific
areas as examples of use in parameter optimisation and in
discharge prediction mode.

2.   An investigation into the appropriate specification of
initial hillslope water conditions has been completed.
Mathematical and, to a greater extent, hydrological
considerations indicate the use of appropriate 'run-in' times
before events of interest are introduced. Approximations to
initial saturated zone extent based on limited data have been
investigated, and effects of finite element mesh discretisation
taken into account.

1

3.   Automatic optimisation techniques have been implemented for
the IHDM, and an analysis of the error function of the model is
under investigation, the structure of such error surfaces being
in general little known.   This is to be combined with an analysis
of the correlation structure of model parameters, as a potential
aid to calibration procedures.

4.   New modelling initiatives have taken the form of initial
attempts at partially-distributed formulations rather than (as
above) numerical solution of partial differential equations.
These have taken into account those elements shown in practice to
be important in the latter, whilst aiming for less complexity and
more efficient run times.   These models may be seen as time-area
formulations with spatially and temporally different
distributions.   Key problems at present are the use of a
manageable number of parameters, details of continuity and the
apparent unsuitability of some standard optimisation procedures.

Future strategies seen at present as important include (i) the
further exploration of partially-distributed physically-based
methodologies, (ii) the planned feasibility studies of the use of
the p.d.e.-type model in slope stability studies via the
prediction of pore water distributions, and (iii) discussion of
the role of and modifications to physically-based modelling in -
meeting the current widespread interest in environmental impact
assessment via large scale hydrological modelling.

REMAINING MILESTONE DATE(S)	DELIVERABLE
Sept 1992	Report contribution: IHDM preprogram sensitivities
Sept 1993	Report contribution: Assessment of pore water prediction by IHDM in slope stability analysis

DELAYED MILESTONE(S):-

TARGET	REVISED DATE	COMMENTARY ON PROGRESS

DISSEMINATION DETAILS FOR 1991

(a) Journal Publications

Watts, L G and Calver, A (1991) Effects of spatially-distributed rainfall on runoff using a physically-based model. Nordic Hydrology, 22, 1-14.

Calver, A and Wood, W L (1991) Dimensionless hillslope hydrology. Proceedings of the Institution of Civil Engineers, Part 2, 593-602.

Binley, A M, Beven, K J, Calver, A and Watts, L G (1991) Changing responses in hydrology: assessing the uncertainty in physically-based model predictions. Water Resources Research, 27, 1253-1261.

Wood, W L and Calver, A (in press) Initial conditions for hillslope hydrology modelling. Journal of Hydrology.

Effects of Spatially-Distributed Rainfall

on Runoff for a Conceptual Catchment

L. G. Watts and A. Calver

Institute of Hydrology, Wallingford, U.K.

A physically-based rainfall-runoff model is used to investigate effects of moving storms on the runoff hydrograph of throughflow dominated idealised catchments. Simulations are undertaken varying the storm speed, direction, intensity, the part of the catchment affected by rainfall, and the spatial definition of rainfall zones. For a 100 km^2 catchment, under the circumstances investigated, an efficient spatial resolution of rainfall data is around 2.5 km along the path of the storm. Storms moving downstream produce earlier, higher peaks than do storms moving upstream. Error is most likely to be introduced into lumped-rainfall predictions for slower storm speeds, and the likely direction of this error can be specified. Differences in magnitude of peak response between downstream and upstream storm directions reach a maximum at a storm speed and direction similar to the average peak channel velocity. These results are qualitatively similar to those reported for overland flow dominated catchments, but differences in peak runoff between downstream and upstream storm directions are much smaller where rainfall inputs are modified by a period of hillslope throughflow.

Introduction

Distributed rainfall-runoff models offer the facility of incorporating precipitation fields which vary over time and space. This paper uses a physically-based distributed rainfall-runoff model to investigate systematically the effects of moving storm rainfall on the catchment hydrograph. Attention is focussed on conditions

1

under which hillslope hydrographs are generated by throughflow, which subsequently becomes lateral input to a channel network. Hydrological effects of storm parameters are discussed and certain guidelines suggested for the efficient incorporation of spatially distributed precipitation in modelling applications.

Ngirane-Katashaya and Wheater (1985) reported that there are few studies quantifying the effects of storm characteristics on runoff response. Further, previous studies are almost exclusively of urban or overland flow dominated catchments, partly because of the practical importance to urban storm drainage and partly because the rapid response of an urban catchment is considered most sensitive to variations in rainfall. The present study addresses the paucity of quantitative studies on the effects of storm characteristics on throughflow dominated catchments.

The effects of storm characteristics on channel network hydrographs have been studied using mathematical models of synthetic catchments (for example, Ngirane-Katashaya and Wheater 1985) and of real catchments (Niemczynowicz 1988), and laboratory models (for example, Shen *et al.* 1974). Ngirane-Katashaya and Wheater (1985) used a distributed runoff model with an idealised urban network to study the effects of storm velocity, catchment area, storm direction and response parameters on the runoff hydrograph. Surkan (1974) examined a non-urban model, but the only treatment of storage was by a specified delay time for release of water from a subarea experiencing rainfall. Shen *et al.* (1974) developed a laboratory model with an impervious basin to examine the effects of the intensity, duration, velocity and non-uniform areal distribution of rainfall together with catchment size, shape and slope. The main finding of all these studies was that peak discharge from a storm moving downstream exceeds that from a storm moving upstream, but that the degree of this "maximal directional bias" (Niemczynowicz 1984) varies greatly between studies depending on catchment characteristics. Niemczynowicz (1988), using data from the Lund area of Sweden, stressed the benefits of using storm movement parameters to complement inadequate rainfall data and, conversely, the problems in not incorporating such information.

Methodology

Model Description
The model used in the present investigations is the Institute of Hydrology Distributed Model (IHDM). Details of the structure of this model are provided by Beven *et al.* (1987). Essentially, surface and subsurface equations of flow are solved numerically for appropriate spatially-distributed hillslope and channel components of a catchment.

2

Effective precipitation falling on a catchment hillslope component becomes overland flow or enters soil moisture storage depending on the time-dependent hydraulic conductivity and water content of the surface soil layers. Saturated and unsaturated subsurface flow occur in a Darcian manner. Taking into account mass conservation, then

$$\frac{\partial \theta}{\partial t} - \frac{\partial}{\partial x}(k_x \frac{\partial \phi}{\partial x}) - \frac{\partial}{\partial z}(k_z \frac{\partial \phi}{\partial z}) = 0 \qquad (1)$$

for unit width of hillslope, without source and sink terms, where x is the horizontal distance from the drainage divide, z is the vertical elevation (above an arbitrary datum), t is time, ϕ is hydraulic potential, θ is the volumetric soil water content and k_x, k_z are hydraulic conductivities in the x, z directions respectively. With θ expressed in terms of ϕ, Eq. (1) is solved numerically for ϕ using a Galerkin finite element method in the two space dimensions and a finite difference time stepping scheme. Lateral contributions to the channel network from hillslope flow are calculated from the potential excess over saturation using the method of Lynch (1984).

Channel flow, comprising this lateral inflow, channel precipitation and any upstream input, is modelled as a kinematic wave. Thus

$$\frac{\partial Q}{\partial t} + c \frac{\partial Q}{\partial y} - ci = 0 \qquad (2)$$

for unit width, where Q is discharge, y is down channel-distance, i the lateral inflow rate per unit down-channel length, and c is the kinematic wave velocity, defined by dQ/dA, where A is cross-sectional area of flow. Eq. (2) is solved by a finite difference scheme. Catchments are divided into appropriate hillslope and channel components and the calculations undertaken in a downstream sequence.

Catchment Geometry and Physical Parameters

The sensitivity of the model to spatially-distributed rainfall was tested for the idealised channel network of Fig. 1a in which the relationship between distance up the channel network from the outflow point and the number of contributing channels at that distance is close to linear. To reduce computation costs, it was assumed that each channel received contributions from two hillslopes of identical geometry. Since different rainfall distributions were assigned to different zones within the catchment (see below), this allowed the use of just one hillslope simulation to represent each distinct rainfall zone.

The dimensions of the hillslope components of the model were defined by reference to the number of similar channel reaches in an assumed 100 km² drainage area: each hillslope plane was 1,000 m in length along the channel and 1,136 m from channel to divide with a gradient of 0.09. The plane was discretised using 6 nodes vertically and 308 nodes horizontally. The vertical element dimension was 0.2 m throughout. The horizontal element dimensions increased, with ratio 1.1, from 0.2 m near the channel to a maximum of 4.0 m towards the divide.
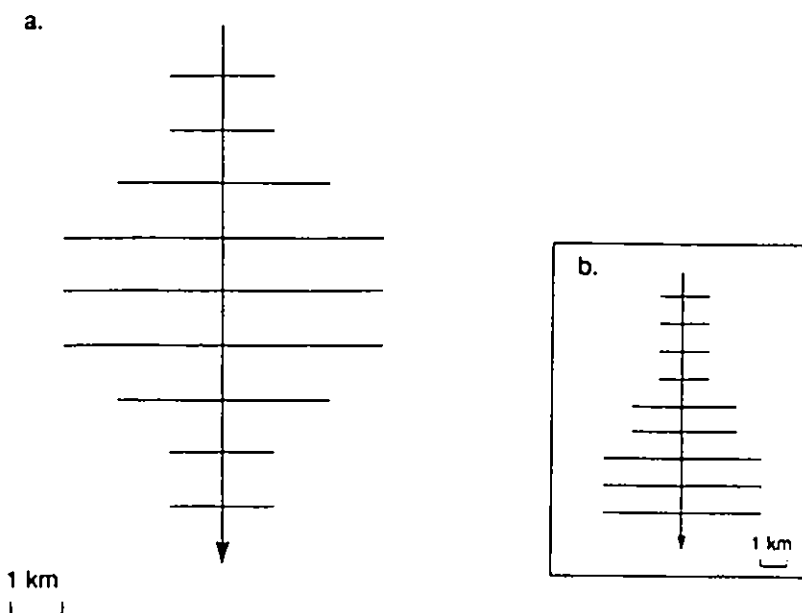
3

a.

b.

1 km

1 km

Fig. 1. a) Channel network. b) Modified channel network.

This scale is one at which significant differences in the time of response of different parts of the catchment may be expected, whilst also being a scale at which a substantial proportion of the catchment is likely to be subject to a particular storm, such that hillslopes are involved in hydrograph generation rather than merely providing a baseflow contribution to a channel floodwave routed through a network.

Investigation of effects of storm characteristics can be undertaken for a range of values of physical properties of hillslopes and channels. It was felt most appropriate, in a concise study, to concentrate on typical, non-extreme parameter values, representative of humid temperate landscapes. These values were selected on the basis of general hydrological experience together with information from previous modelling using the IHDM (see, for example, Calver 1988).

The soil was assumed to be uniform in physical properties, to have a constant depth of 1.0 m and to overlie impermeable bedrock. A porosity of 0.4 was assumed and the soil moisture characteristic and relationship of hydraulic conductivity to unsaturated pressure potential were defined as those of a medium texture loam (Clapp and Hornberger 1978). Saturated hydraulic conductivity k_s can vary, in measurement and in model calibration, over a very large range. Since the model has been seen to be very sensitive to this parameter, two values of saturated hydraulic conductivity were employed, varying by an order of magnitude, namely 0.1 and 1.0 m hr^{-1}; these values of k_s were applied in both x and z directions. The

4

7

initial pressure potential on the hillslope was set everywhere at −0.3 m water, which defined an initial water content of 36 % by volume and a hydraulic conductivity of approximately one third of the saturated value. Sufficient simulation run-in time was allowed for the establishment of steady numerical and hydrological conditions.

The lengths of channel reaches and their linkages followed from the overall network configuration. Each channel was discretised by 51 equidistant nodes along a 1,000 m length. Channel slope was standardised at 0.02, the channel cross-section was rectangular with a width of 1.0 m, and the rating curve was of the form

$$Q = r\, s^{0.5}\, A^{1.5} \tag{3}$$

where s is slope and r a roughness coefficient, here set at 50,000 hr^{-1}. Over the range of discharge of interest here this is equivalent to a Manning's n value of 0.035.

Storm Characteristics

For a given storm a constant intensity was maintained for a particular duration. Intensities were taken as representing effective precipitation. For much of the United Kingdom, a 1 hr duration storm with a return period of 5 years has a typical intensity of 0.02 m hr^{-1} (Natural Environment Research Council 1975). For the present study intensities varying between 0.002 and 0.02 m hr^{-1} were considered. Storm duration was taken as equal to 100 time steps except where duration was varied with intensity to ensure constant total rainfall. Time steps were of 50 seconds duration, as explained below.

In a study of storms in the United Kingdom, Marshall (1980) found that 86 % of storms had speeds of less than 16.7 m s^{-1}. It is intuitive, and confirmed in this study, that sensitivity of runoff to storm direction decreases at high storm speeds. For these reasons, storm speeds of 1, 2 and 10 m s^{-1} were investigated.

The present study investigated the degree of subdivision of a catchment into zones of like time-distribution of rainfall necessary to reasonably represent real storm characteristics. In each zonation scheme, subdivision was on the basis of zonation perpendicular to storm direction, an equal number of plane and channel components being assigned to each zone. Storm movement was simulated by displacing the time of onset of rainfall for subsequent zones with respect to the time of storm arrival for the first zone.

An analysis of effects of spatially distributed rainfall was also performed on a smaller catchment area of 1 km^2 for which subdivision into 2 zones was thought sufficient. Plan dimensions in this case were reduced by a factor of 10. A model time step of 50 seconds was dictated by the travel time between the centres of the 2 zones of the small catchment, 500 m apart, for the fast storm of 10 m s^{-1}. This small time step was utilised for both catchment areas from the onset of rainfall. However, prior to rainfall a larger time step of 0.5 hr was sufficient for solution stability.
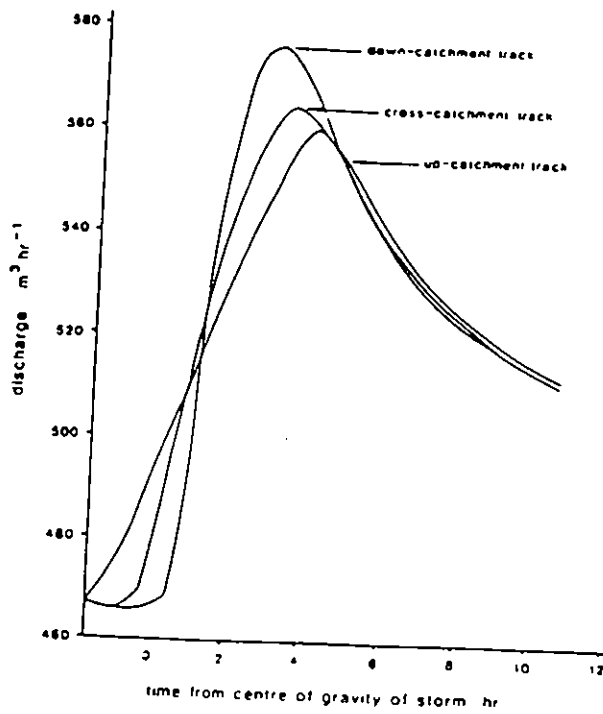
5

8

Fig. 2. Catchment hydrographs for different storm directions.

Results

Hillslope Water Content and Hydrograph Response

For the 100 km² catchment, the storm of 0.002 m hr⁻¹ intensity and 100 time steps of 50 seconds duration promotes a rise from 0.27 to 0.30 m in the depth of satura-tion at the base of the soil profile. In the case of $k_s = 0.1$ m hr⁻¹, total water storage on the hillslope increases slightly over the course of the simulation: for the $k_s = 1.0$ m hr⁻¹ case, which promotes greater discharges, overall slope water content de-creases slightly.

Fig. 2 shows the hydrographs at the network outflow point for the $k_s = 0.1$ m hr⁻¹ case with the 1 m s⁻¹ storm speed. The high baseflow component, typical of subsurface flow dominated catchments, is apparent. The $k_s = 1.0$ m hr⁻¹ case generated a baseflow of 4,487 m³ hr⁻¹. The rainfall-induced rise in the hydrograph occurs first for the upstream storm direction, due to proximity to the outflow point of the earliest rainfall and lastly for the downstream storm direction because rain-fall begins at the furthest point from the outflow.

Discretisation of Catchment Rainfall

In order to establish an appropriate number of zones required for spatially-distri-
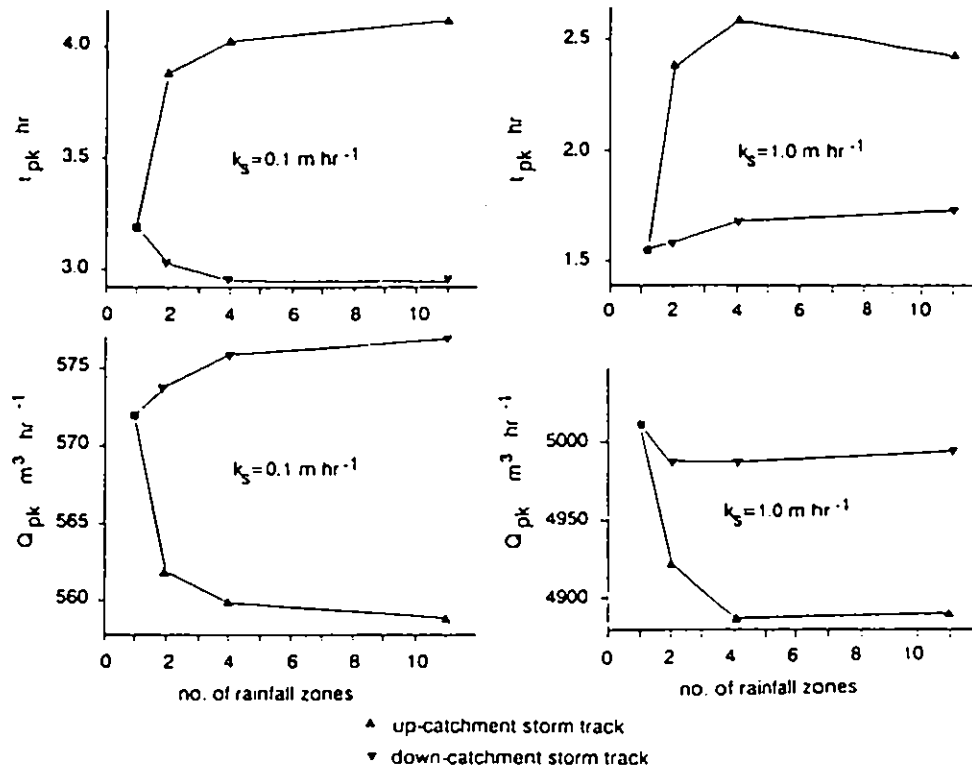
6

9

Fig. 3. Effects of number of rainfall zones on peak discharge and time to peak.

buted rainfall representation, simulations were performed to determine the time to peak t_{pk} and peak discharge Q_{pk} for catchment subdivisions into 1, 2, 4 and 11 zones. The time to peak was defined as the time from the centre of gravity of the storm, considering the rainfall in all zones. Results are presented in Fig. 3 for the slower storm of 1 m s^{-1}, with 0.002 m hr^{-1} intensity and 100 time steps duration, which generates larger differences in t_{pk} and Q_{pk} than the faster storms.

The magnitude and timing of peaks tend to approach constant values as the number of zones increases, for both downstream and upstream storm directions. Peaks for the downstream storm direction are both earlier and higher because the flow peak generated by rain falling in the upstream part of the catchment arrives in the downstream part of the catchment as peaks generated by rain falling in the downstream part of the catchment are occurring, and thus flows are augmented. Peaks for $k_s = 1.0$ m hr^{-1} are earlier and higher than for $k_s = 0.1$ m hr^{-1} because the higher conductivity promotes the rapid removal of a greater volume of water from hillslope storage. These results suggest that for this size of catchment the use of 4 zones provides an efficient representation of the tracking of a storm. Subsequent simulations were thus performed using the 4 zones scheme.
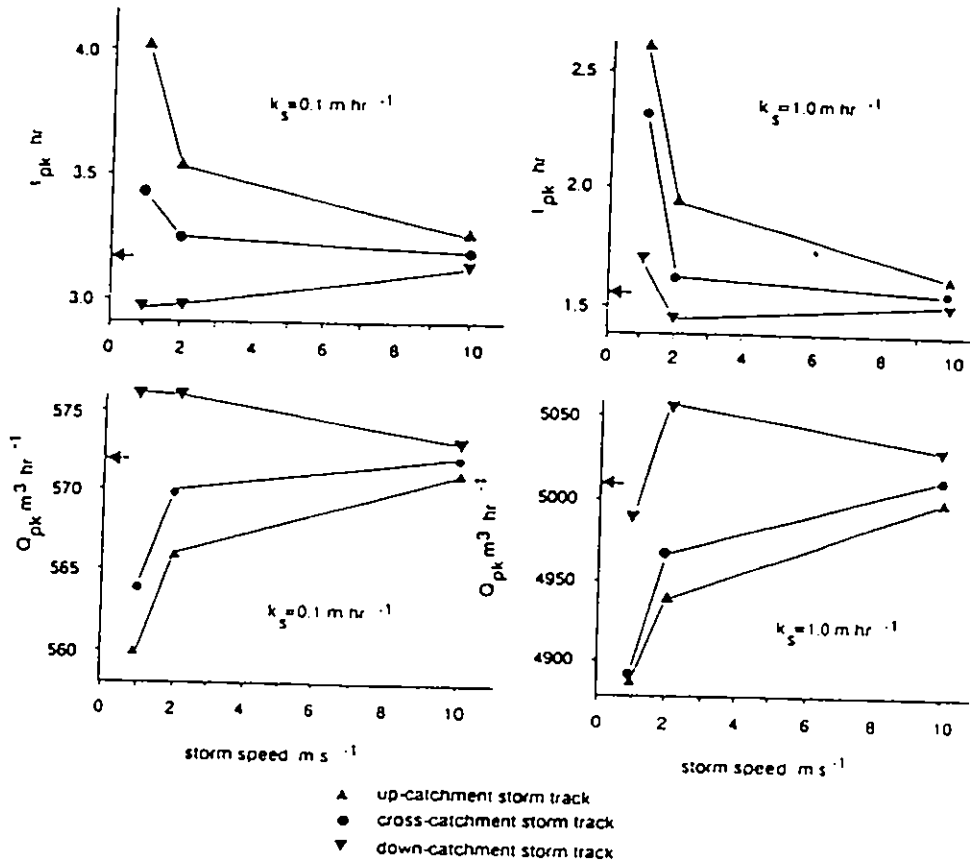
7

Fig. 4. Effects of storm velocity on peak discharge and time to peak. Arrows against vertical axes indicate lumped rainfall results.

Effects of Storm Velocity

Fig. 4 shows the effect of storm velocity on t_{pk} and Q_{pk}. As storm speed increases, the differences in t_{pk} and Q_{pk} between downstream and upstream storm directions decrease and converge on the results of the 1 zone simulations of catchment-lumped rainfall.

For $k_s = 1.0$ m hr^{-1}, a greater difference in Q_{pk} between upstream and downstream storm directions occurs for the 2 m s^{-1} storm compared with either the 1 m s^{-1} or 10 m s^{-1} storm speeds. The 2 m s^{-1} storm produced a mean cross-sectional velocity, averaged down the main channel, of around 2.1 m s^{-1}. For $k_s = 0.1$ m hr^{-1}, the greatest difference in Q_{pk} between upstream and downstream storm directions occurs for a storm speed less than 1 m s^{-1} (Fig. 4). A further simulation showed that a 0.5 m s^{-1} storm generated an averaged peak in mean cross-sectional velocity down the main channel of around 0.54 m s^{-1}. These results suggest that a storm speed which promotes a large difference between peaks generated by up-

8

stream and downstream storm directions is similar in magnitude to the average channel velocity. This effect is the "maximal directional bias" referred to by Niemczynowicz (1984).

On the smaller catchment area of 1 km^2, for the 1 m s^{-1} storm and for both k_s values, there was little difference in t_{pk} and negligible difference in Q_{pk} for downstream compared with upstream storm directions.

To investigate the effect of a different network on model results, the original network was modified by repositioning channels closer to the outflow point (Fig. 1b). For the 1 m s^{-1} storm, differences in t_{pk} and Q_{pk} between the two networks for a given storm direction were almost an order of magnitude smaller than the differences in t_{pk} and Q_{pk} between storm directions for either network.

Effects of Storm Intensity

Fig. 5 shows results of investigating effects of a range of intensities of moving storm rainfall, using the 1 m s^{-1} storm velocity since this showed greatest differences for different storm directions. In Fig. 5a the same storm rainfall total is maintained as in the previous simulations whilst intensity and therefore duration are changed, whereas in Fig. 5b the same duration is maintained whilst intensity and therefore rainfall total are varied.

Fig. 5a suggests a maximum value of peak discharge is approached at a decreasing rate as intensity is increased. Differences in peak flow between upstream and downstream storm directions are maintained over the intensity range. Time to peak is little altered by varying intensity.

In Fig. 5b increasing intensity is associated with an increase in peak discharge at a slightly increasing rate over the range considered. Differences in peak discharge for upstream and downstream storm directions are increased with increasing intensity. The time to peak maintains a roughly constant difference between upstream and downstream storm directions over the range of intensity. The difference in behaviour between the two hydraulic conductivity cases appears to reflect a limit on the trend towards greater rates of water input to the hillslope shortening the time to peak response: this limit appears to have already been reached at a relatively low rainfall intensity under conditions of generally faster water movement of the higher conductivity case.

Effects of Spatial Extent of Storm

Spatial variation not only in the timing of an event across a catchment but also in total rainfall was investigated. The same intensity and duration of storm rainfall was employed as in the majority of the above simulations (that is, 0.002 m hr^{-1} for 100 time steps) with a 1 m s^{-1} storm velocity. This was applied to 50% of the catchment, the particular 50% being distributed in a variety of locations with respect to network orientation and storm direction (Fig. 6). Total water input into the catchment is thus halved compared with most earlier simulations, while the
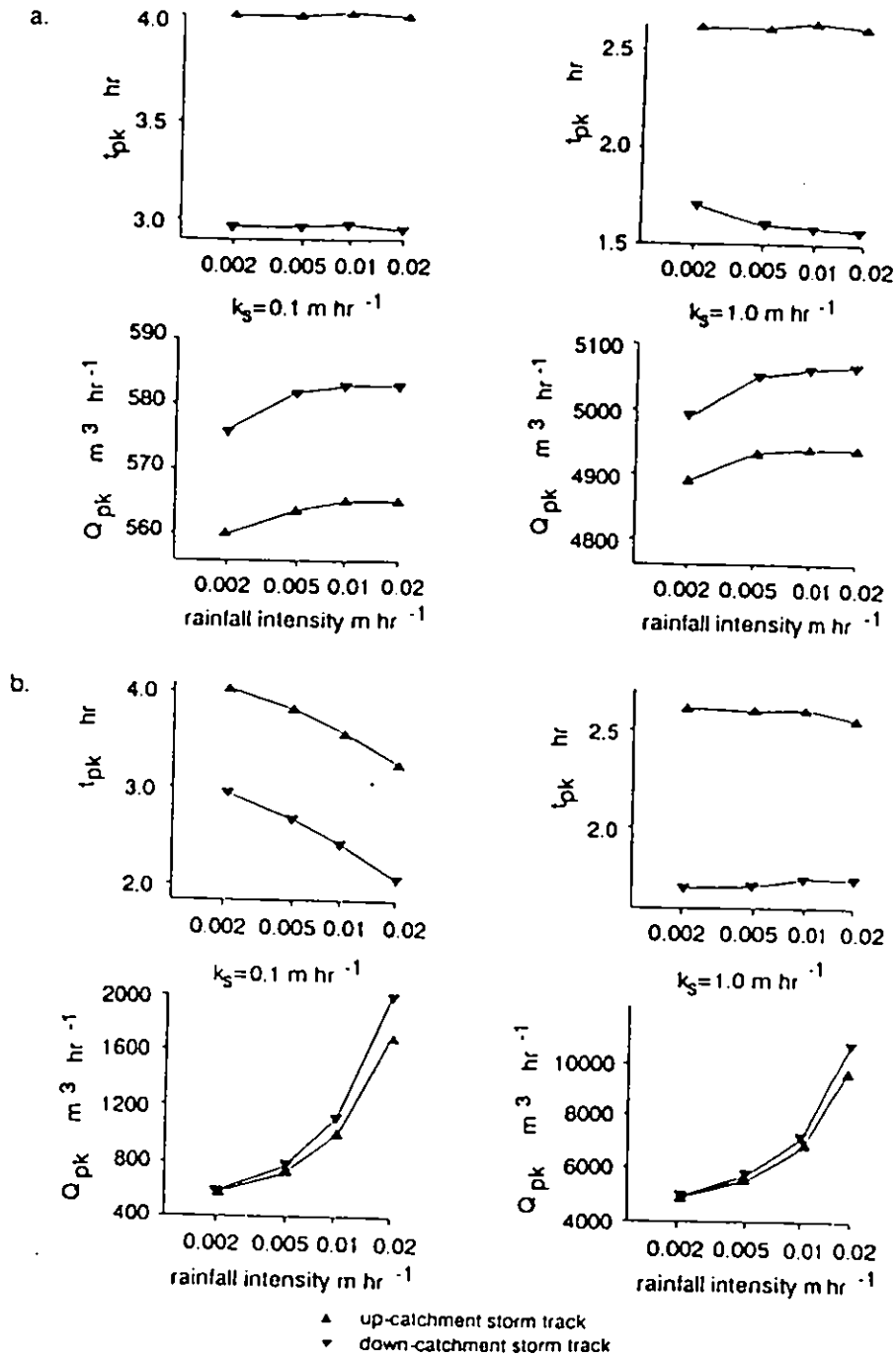
9

Fig. 5. Effects of rainfall intensities on peak discharge and time to peak.
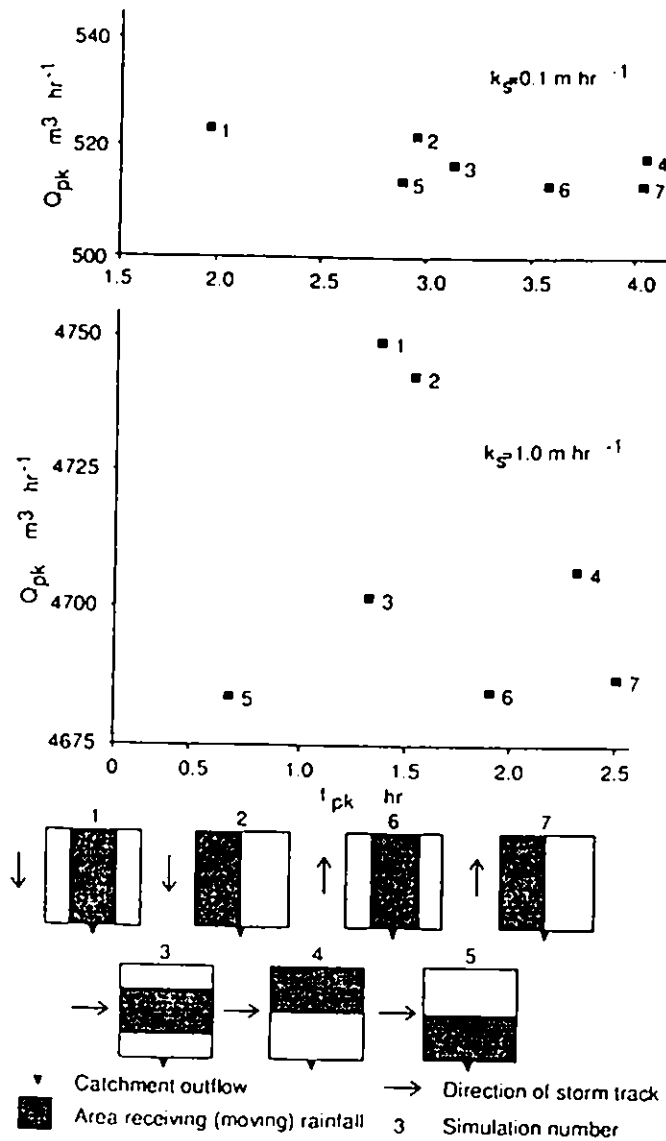a) Constant rainfall total. b) Constant rainfall duration.

Fig. 6. Effects on peak discharge and ti ne to peak of rainfall affecting specific half-catchment areas.

hillslope discharge hydrograph is unchanged for those areas which receive rainfall.

The rise above baseflow for storms affecting half the catchment is a little over half the rise for storms affecting the whole catchment. Timing of peak is earlier for half-catchment storms than whole-catchment storms for $k_s = 1.0$ m hr^{-1} and is either earlier or later for $k_s = 0.1$ m hr^{-1}, depending on which half of the catchment is affected.

11

14

For storms affecting half of the catchment (Fig. 6), downstream storm directions (cases 1 and 2) promote higher peaks than do upstream storm directions (cases 6 and 7). The different distribution of channel links to the main channel in central and side halves does not produce a simple relationship between position of half-catchment receiving rain and the magnitude of the peak response. The cross-catchment storm direction shows peak discharges intermediate between upstream and downstream storm directions for central and upper-catchment halves (cases 3 and 4), but for the lower-catchment half (case 5) the peak flow is very similar to the upstream storm direction case. A small increase in peak is noted for storm locations further from the catchment outfall because augmentation of peak flows from each of the four rainfall zones occurs for the upper-catchment rainfall case but not for the lower-catchment rainfall case.

The time to peak discharge for the half-catchment storms is shorter for downstream than upstream storm directions, as with the full-catchment storms, and times to peak for $k_s = 0.1$ m hr^{-1} are generally longer than for $k_s = 1.0$ m hr^{-1}.

For a given storm direction, the central half cases consistently produce slightly quicker responses than the side halves because of the more numerous shorter routes to the main channel in the former case. For the cross-catchment storm direction, times to peak vary considerably with the location of the 50% of the catchment receiving rain since there are greater differences in channel linkages to the catchment outfall for the cross-catchment storm direction than for the upstream or downstream storm directions.

Concluding Remarks

The key findings of this study are summarised below, bearing in mind that any investigation using a specific model and specific parameter values should acknowledge limitations on the generality of its conclusions.

For the 100 km^2 drainage area considered, peak discharge for the downstream storm direction was earlier and higher than for the upstream storm direction, with the cross-catchment storm directions generating intermediate results. Qualitatively, directional differences were maintained over a range of intensities and precipitation totals. For storms occurring on only part of the catchment, the same trends were seen, but with complications introduced by the particular area of catchment concerned.

For a 0.002 m hr^{-1} storm of 1.4 hr duration the maximum difference in storm hydrograph rise above baseflow between upstream and downstream storm directions occurred at a storm speed of 0.5 m s^{-1} and gave a 22% difference (expressed as a percentage of upstream storm direction rise) for the lower hydraulic conductivity case ($k_s = 0.1$ m hr^{-1}). For the higher conductivity ($k_s = 1.0$ m hr^{-1}) and

12

15

generally higher flow case, the corresponding storm speed was 1.0 m s^{-1} and the difference was 29 %. As storm speed increased, peak and time to peak values converged towards values obtained for the catchment-lumped rainfall case. The differences between upstream and downstream storm directions are much lower than for most overland flow dominated studies: though the results are qualitatively similar, precipitation variability is considerably filtered by subsurface hillslope flow.

For a 1 km^2 catchment the above effects of distributed precipitation are very greatly reduced. It may be expected in general that storm characteristics have more scope for affecting the runoff hydrograph in larger catchments, though there would appear to be a limit to this process at a scale at which only a small part of a catchment is likely to be directly affected by the rainstorm.

If distributed precipitation data are not available in runoff prediction and catchment-lumped data are used, error is most likely to arise in the case of the lower storm speeds. For the case of the lumped data being of the same precipitation intensity and same total catchment rainfall, the direction of error is most likely to be an underprediction of peak discharge and overprediction of time to peak in the case of storms moving downstream, and an overprediction of peak discharge and underprediction of time to peak for upstream or cross-catchment storm directions. It is appreciated that variations in catchment geometry and physical parameters may in cases outweigh these considerations.

For convective rainfall, the finest available definition of rainfall may be desirable for modelling. For the scale, hydrological environment and frontal regimes considered here, it appears desirable to take account of distributed rainfall data at a resolution of about 2.5 km in the direction of storm movement. There is not a great deal of predictive gain, and there may be considerable disadvantage in computational effort, to include precipitation data to a finer resolution for catchments at this scale. Since a 2 km grid resolution is commonly used for deriving rainfall data from radar measurement, these investigations underline the potential benefit of complementing hydrograph prediction using physically-based models with radar-derived precipitation fields.

Acknowledgements

13

References

Beven, K., Calver, A., and Morris, E. M. (1987) The Institute of Hydrology Distributed Model, Institute of Hydrology Report No. 98.

Calver, A. (1988) Calibration, sensitivity and validation of a physically-based rainfall-runoff model, *J. Hydrol. Vol. 103* (1/2), pp. 103-115.

Clapp, R. B., and Hornberger, G. M. (1978) Empirical equations for some soil hydraulic properties, *Water Resour. Res., Vol. 14* (4), pp. 601-604.

Lynch, D. R. (1984) Mass conservation in finite element groundwater models, *Adv. Water Resour., Vol. 7* (2), pp. 67-75.

Marshall, R. J. (1980) The estimation and distribution of storm movement and storm structure, using a correlation analysis technique and raingauge data, *J. Hydrol., Vol. 48* (1/2), pp. 19-39.

Natural Environment Research Council (NERC) (1975) Flood studies report. 5 volumes, London.

Ngirane-Katashaya, G. G., and Wheater, H. S. (1985) Hydrograph sensitivity to storm kinematics, *Water Resour. Res., Vol. 21* (3), pp. 337-345.

Niemczynowicz, J. (1984) Investigation of the influence of rainfall movement on runoff hydrograph. Part 1 – Simulation on conceptual catchment, *Nord. Hydrol., Vol. 15* (2), pp. 57-70.

Niemczynowicz, J. (1988) The rainfall movement – a valuable complement to short-term rainfall data, *J. Hydrol., Vol. 104* (1-4), pp. 311-326.

Shen, Y. Y., Yen, B. C., and Chow, V. T. (1974) Experimental investigation of watershed surface runoff, A contribution to the International Hydrological Decade, Hydraulic Engineering Series No. 29, University of Illinois, pp. 1-215.

Surkan, A. J. (1974) Simulation of storm velocity effects on flow from distributed channel networks, *Water Resour. Res., Vol. 10* (6), pp. 1149-1160.

Address:
Institute of Hydrology,
Wallingford,
Oxfordshire OX10 8BB,
United Kingdom.

14

Changing Responses in Hydrology: Assessing the Uncertainty in Physically Based Model Predictions

A. M. BINLEY AND K. J. BEVEN

*Centre for Research on Environmental Systems, Institute of Environmental and Biological Sciences
University of Lancaster, Lancaster, England*

A. CALVER AND L. G. WATTS

Institute of Hydrology, Wallingford, Oxon, England

Due to the large number of model parameters requiring calibration and their inherent uncertainty, the practical application of physically based hydrologic models is not a straightforward task and yet has received inadequate attention in the literature. This work investigates the determination and usefulness of a measure of predictive uncertainty in a particular distributed physically based model, using the methods of Rosenblueth (1975) and Monte Carlo simulation, in an application to an upland catchment in Wales. An examination of the role of predictive uncertainty in assessing the hydrological effect of land use change is also made. The results of the study suggest that, even following parameter constraint through calibration, the predictive uncertainty may be high and can be sensitive to the effects of land use change.

INTRODUCTION

Physically based distributed models offer the capability, in theory, of predicting the response of catchments based on knowledge of a catchment's physical properties. In principle, such models can be calibrated on the basis of field measurements alone, allowing prediction of the hydrological responses of ungauged catchments and of the changing responses resulting from changes in land characteristics [*Beven and O'Connell*, 1982]. In practice, however, there are many problems associated with calibration on the basis of field measured parameters. Many of the currently available distributed models are variants on the structure proposed by *Freeze and Harlan* [1969] in which descriptive partial differential equations for the different flow processes are solved by approximate numerical methods using a discrete representation of the catchment as a finite difference or finite element grid. Parameter values are required by the models at every grid element and, for a solution that is stable and convergent with the original differential equation, a large number of grid elements may be required. Thus, the number of parameter values required is far too great for determination by experiment, even on intensively monitored research catchments. Indeed, in most cases, the experimental techniques to measure or estimate the parameter values at the scale of the grid element do not exist (see discussion of *Beven* [1989]). The common approach to applying physically based models is to treat the model in a similar manner to lumped conceptual models and perform some calibration procedure over a number of observed events [e.g., *Bathurst*, 1986]. Computational considerations may require that the length of the calibration period is small. Such calibration may also be used to compensate for errors in the observed input data and discharges, poorly known boundary condi-

tions and unknown spatial heterogeneity effects, and imperfect process approximation by the model equations [see *Stephenson and Freeze*, 1974].

The calibration of physically based models is not a straightforward task due to the large number of model parameters involved and the computational requirements of making multiple runs of such models. A set of calibrated parameters will generally represent one possible combination that, in conjunction with the particular model structure and solution scheme used, produces a response similar to that observed. It is unlikely that, for a particular model structure, this set of values is unique in this respect. Also, it should not be expected that this set of parameter values will give equally good results when used with a different model structure, even though the model may purport to solve the same equations and the model parameters may have the same names.

Physically based models are best suited to research applications, in which they are used to explore the implications of making different assumptions about the nature of hydrological systems. They are less well suited to exploring the implications of making different assumptions about the nature of specific hydrological systems, and possible future changes to a system. There are, however, increasing requirements for such predictions and current physically based models are already being used in this way. It is our view that in carrying out such studies, the predictions of the model must be associated with a realistic assessment of the uncertainty arising from problems of model calibration.

This paper continues the earlier work of *Rogers et al.* [1985] by investigating the determination and usefulness of predictive uncertainty in the Institute of Hydrology distributed model (IHDM) in an application to an upland catchment in Wales. An examination of two methods for estimating predictive uncertainty is made together with a case study of using the level of uncertainty to assess predictions of changing hydrological responses as a result of changes in land use.

18

TABLE 1. Storm Characteristics for the Gwy Catchment

Storm	Date	Total Rainfall, mm	Maximum Intensity, mm h^{-1}	Peak Flow, m^3 s^{-1}
1	Nov. 17–19, 1981	80.51	9.17	8.0
2	Dec. 8–10, 1983	98.23	8.72	7.2
3	Jan. 27–29, 1983	111.44	8.60	6.1
4	Oct. 5–7, 1980	94.78	13.34	10.5
5	Jan. 13–15, 1981	74.91	11.56	8.3
6	Feb. 11–13, 1976	107.25	10.43	8.5
7	Nov. 17–19, 1978	124.18	8.74	7.6
8	Aug. 5–7, 1973	121.77	25.66	16.8*

*estimated

INSTITUTE OF HYDROLOGY DISTRIBUTED MODEL

The Institute of Hydrology distributed model, version 4 (IHDM4) employs established flow equations in a linked and spatially distributed manner to cover the range of runoff processes in a catchment. A catchment is represented as a number of hillslope planes and channel reaches. Surface flows on each hillslope and stream channel flow are modeled in a one-dimensional sense by a kinematic wave equation solved by a finite difference scheme. Subsurface flow, both saturated and unsaturated, is modeled by the Richards equation, incorporating Darcy's law and mass conservation considerations. It is solved by a two-dimensional (vertical slice) Galerkin finite element scheme with allowance for varying slope widths and slope angles to account for slope convexity/concavity and convergence/divergence. Linkages are made between the different flow types: Hillslope overland flow can arise from saturation excess and/or infiltration excess of the soil material, and saturated zones within the soil of the lower hillslopes provide lateral flow contributions to the stream system. Full details of the IHDM4 structure are given by Beven et al. [1987]. We note in passing that the earlier work of Rogers et al. [1985] used version 3 of the IHDM in which hillslope geometry was less flexibly defined and where the subsurface flow equation was solved by finite difference methods. A greater proportion of modeled flow in the example used for the IHDM3 Rosenblueth [1975] analysis was surface flow than is the case in the current study using IHDM4 (see below).

Effective precipitation input into the IHDM is provided by a preprogram [Watts, 1988], the first part of which modifies automatic weather station (AWS) data into a form consistent with spatial differences in slope, altitude and aspect throughout a catchment. The second part of the preprogram models the processes of interception, evapotranspiration, snowmelt and throughfall, though not stemflow. Potential evapotranspiration is determined using a Penman-Monteith equation [Monteith, 1965]. Evaporation of intercepted water is calculated from vegetation characteristics, changes in canopy

storage over time being calculated from a modified Rutter interception model [Rutter et al., 1971].

DESCRIPTION OF THE STUDY CATCHMENT AND MODEL CALIBRATION

The Gwy catchment at the head of the River Wye in central Wales has a drainage area of 3.9 km^2. It is an upland area of impermeable bedrock, predominantly shallow soils and grassland vegetation where steamflow is derived from throughflow, natural soil pipe flow and some overland flow. The Gwy has a largely complete flow record since 1973. Catchment rainfall has been gauged since 1973 and an automatic weather station has been operative nearby from 1975. In using the IHDM on the Gwy catchment, the drainage area was divided into five sections of hillslope and three reaches of channel for which flows were individually and sequentially modeled. The topographic configuration was derived from a 1:5000 survey. Grids of calculation points for numerical solutions were chosen for efficient discharge prediction [Calver and Wood, 1989].

Five events of recurrence interval between 1 and 10 years were used as calibration storms; three further storms were used as test events (see Table 1). The shapes of the rising and falling limbs of the calibration hydrographs were not necessarily simple. No periods of snowfall or snow cover were considered in the calibration or validation events. For the Gwy catchment the nearest AWS is at Eisteddfa Gurig (elevation 510 m, approximately 1.5 km distant from the Gwy). A complete AWS data set was available from Eisteddfa Gurig for storms 2, 3, 4 and 6. However, for storms 1, 5, and 7 the Eisteddfa Gurig AWS data sets were incomplete and data from Cefn Brwyn AWS (elevation 355 m, approximately 2.8 km distant from the Gwy) were used instead. Rainfall data were available from a gauge in the Gwy catchment and were used in preference to AWS rainfall records.

Interception and evapotranspiration losses calculated by the preprogram ranged from <1% to 13% and were commonly, for the winter storms, <5%. The vegetation in the Gwy catchment is predominantly grassland and was represented by the grass parameters shown in Table 2; these values are based on the work of Calder [1977] and Rutter and Morton [1977].

Physically based models such as the IHDM require a large number of parameter values to be calibrated in applications to real catchments, even where simplifying assumptions (such as homogeneous, isotropic soil characteristics) are made to reduce those requirements. Sensitivity analysis, however, suggests that the simulations are very much more sensitive to some parameters than to others [e.g., Rogers et al., 1985; Calver, 1988]. This knowledge has been used to reduce the parameter optimization problem, so that only four parameters were calibrated by comparing observed and

TABLE 2. IHDM Preprogram Parameters for Grass and Forest

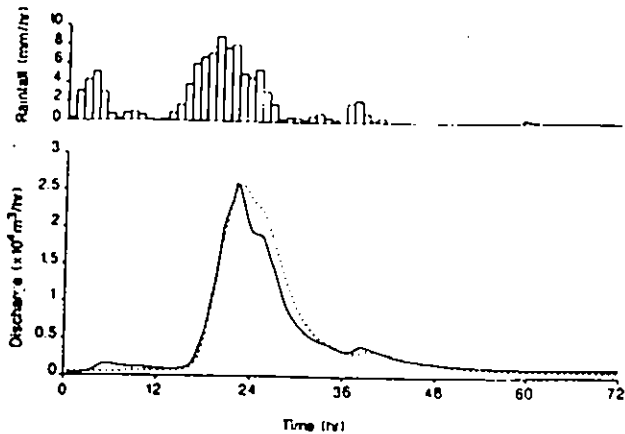| Land Use	Vegetation Height, m	Ground Cover	Interception Capacity, mm	Leaf Area Index	Albedo	Aerodynamic Roughness Length, m	Rutter b, mm	Rutter k, mm h^{-1}
Grass	0.1	0.90	1.0	1.0	0.2	0.01	2.00	0.0342
Forest	10.0	0.92	2.0	2.0	0.1	0.30	1.76	0.0162

Fig. 1. Calibrated and observed outflow rates for storm 2. Dashed line indicates model prediction, solid line indicates observed hydrograph.

simulated discharges, while the other parameters required were fixed on the basis of field estimates. The spatial distribution of the four parameters was considered uniform; thus the parameters represent effective values for the model. The parameters calibrated in this way were the saturated hydraulic conductivity (K_s), the saturated moisture content (θ_s), the initial capillary potential of the soil (ψ_{in}) and an overland flow roughness coefficient (f). Initial soil moisture potential, though not strictly a parameter in this sense, was similarly optimized in the absence of observations. The use of automatic optimization techniques in calibrating physically based models of this type is normally precluded by the computer run times required. Calibration of the IHDM was therefore undertaken based on previous experience of the use of the model in similar physical environments and on hydrological reasoning on inspection of interim results. A least squares error function was used, namely, the sum of squares of the difference between observed and predicted catchment outflow at half-hourly intervals. An example of calibrated and observed response for event 2 is shown in Figure 1.

The relative goodness of fit for the calculation storms expressed as a root mean square error is shown in Table 3.

These are at a similar level to those obtained using the lumped conceptual isolated event model [Natural Environment Research Council, 1975], with parameters optimized using an automatic search routine (unpublished Institute of Hydrology data). Inspection of the interim moisture contents and slope water flows of the calibration events shows that in times of storm response up to some 80% of the channel discharge is contributed by the overland flow kinematic wave modeling, whereas base flows are predominantly or totally derived from subsurface porous medium flow. Field experience suggests that the kinematic wave flow should therefore be seen as approximating the contribution not only of overland flow but also of quick subsurface flow through soil pipes and/or through macropores in general. It appears that the small rainfall prior to the bulk of storms 3 and 5 is not enough to trigger the model's quick response which, if rainfall intensity is insufficient to invoke infiltration excess overland flow, relies on some degree of near-surface saturation promoting saturation excess overland flow. Macropore flow and fast subsurface responses in the field can of course occur without this near-surface saturation.

The very large runoff event of August 5, 1973 (storm 8) was of a magnitude which caused some geomorphological changes to hillslopes and channels. Its return period has been estimated at 50-100 years using the flood studies report [Natural Environment Research Council, 1975] regional frequency curve for Wales (N. W. Arnell, personal communication, 1987). On the basis of the Gwy catchment record alone, which is deemed inadequate in this context, a recurrence interval in excess of 1000 years is indicated. Stage estimates at the Gwy gauging site have been considered unreliable at the height of the event but peak flow near the flume was estimated by a slope-area method as $16.87 \text{ m}^3 \text{ s}^{-1}$ [Newson, 1975]. This estimate assumed some overbank as well as channel flow. This is not overbank flow in the sense of extension over a flood plain but flow against the lower part of hillslopes abutting the channel. No adjustments of channel or hillslope geometry were made when using the model on this event. Wet "winter" initial conditions were used since precipitation had been heavy prior to the main rainfall event. Recorded rainfall data were used as such, without the use of the preprogram, because of the absence of data to run the preprogram appropriately and the expectation that effective

TABLE 3. Calibrated IHDM Parameters for Storms 1-5

Storm	K_s, m h⁻¹	θ_s	ψ_{in}, m	f, m⁰·⁵ h⁻¹	Root Mean Square Error, m³ s⁻¹
1	0.5	0.25	-0.18	3000	0.394
2	0.35	0.30	-0.18	1500	0.345
3	1.50	0.50	-0.18	3500	0.598
4	0.90	0.30	-0.15	4000	0.426
5	1.20	0.35	-0.12	7000	0.598

	K_s, m h⁻¹	θ_s	ψ_{in}, m	f, m⁰·⁵ h⁻¹	
Mean	0.89	0.34	-0.162	3800	
Standard deviation	0.427	0.086	0.024	1806	
Minimum	0.01	0.20	-0.274	100	
Maximum	1.77	0.48	-0.500	7500	

20

TABLE 4. Covariance Matrix for Calibrated IHDM Parameters for Storms 1-5

	K_s, m h^{-1}	θ_s	ψ_{in}, m	f, m$^{0.5}$ h^{-1}
K_s, m h^{-1}	0.182	0.0314	3.78×10^{-3}	473.0
θ_s	0.0314	7.40×10^{-3}	-1.20×10^{-4}	28.0
ψ_{in}, m	3.78×10^{-3}	-1.20×10^{-4}	5.76×10^{-4}	39.6
f, m$^{0.5}$ h^{-1}	473.0	28.0	39.6	3.26×10^{6}

precipitation was a very high proportion of measured rainfall.

EVALUATION OF PREDICTIVE UNCERTAINTY

From the calibration exercise described above, mean parameter values were calculated together with their respective standard deviations as an estimate of model parameter uncertainty conditioned on the calibration (see Table 3). Parameter uncertainty assessed in this way reflects all sources of error in the modeling process, for the range of events considered, including errors resulting from the model structure and observation errors, and the calibration procedures followed. For example, in the procedure used here, based upon physical reasoning in conjunction with a least squares error criterion, the parameter sets show a tendency to emphasize matching of the rising limb and peak flow of each hydrograph, with less weight given to the recession limb.

Due to the necessarily small sample of calibration storms and lack of information suggesting otherwise, the parameters were assumed to belong to normal distributions described by the mean and covariance matrix (see Table 4), with distribution tails removed below and above minimum and maximum parameter values, respectively (see Table 3). The minimum and maximum values were chosen on the basis of past modeling experience to prevent choices of unrealistic values in evaluating model uncertainty.

Various methods exist for obtaining the variability of a response function (in this case the IHDM) given the range of function parameters. Methods based on Taylor series truncation impose restrictions on the response function (for example, continuity of derivatives), and evaluation of derivatives, by either numerical or analytical means, is required. A less restrictive method, Monte Carlo simulation, involves making a large number of realizations of parameter values and thus model responses. Monte Carlo simulation has a number of advantages for problems such as that addressed here. In particular, the technique is readily understood, preserves the nonlinear interactions of the parameters within the model calculations, and is not dependent upon limiting assumptions about an appropriate distribution of parameter values. However, in that it requires a large number of simulations, the approach is computationally intensive in the case of physically based modeling.

For this reason Rogers et al. [1985] adopted the method of Rosenblueth [1975] for their study. Rosenblueth's method has also been used by Guymon et al. [1981] in a probabilistic-deterministic analysis of frost heave. Guymon et al. state a generalized form of Rosenblueth's method, which may be written as

$$E[(y)^N] = \frac{1}{2^m}[(q_{+++ \cdots m})(y_{+++ \cdots m})^N + (q_{-+ \cdots m})$$

$$\cdot (y_{-++ \cdots m})^N + \cdots + (q_{---- \cdots m})(y_{----- \cdots m})^N]$$

where $E[(y)^N]$ is the expected value of the Nth moment of function y, m is the number of parameters, $(y_{+++ \cdots m})^N$ indicates the Nth moment of the function evaluated with the m parameters at either mean plus (+) or mean minus (-) 1 standard deviation and the function q is defined in terms of the correlation matrix ρ as

$$q_{i,j, \cdots m} = 1 + \sum_{g=1}^{m} \sum_{h=1}^{m_i} g'h' \delta_{g,h} \rho_{g,h}$$

where

$$\delta_{g,h} = 0 \qquad g \geq h$$

$$\delta_{g,h} = 1 \qquad g < h$$

and g' and h' are -1 or $+1$ depending on the sign of the permutation of the q function subscript; for example,

$$q_{++-+} = 1 + \rho_{12} - \rho_{13} + \rho_{14} - \rho_{23} + \rho_{24} - \rho_{34}$$

Rosenblueth's method, therefore, allows the approximate determination of mean and variance of the response to be made from knowledge of the simulated responses using mean ± 1 standard deviation values for each parameter. The method requires 2^m simulations, where m is the number of parameters, and thus usually requires considerably less computer time than the Monte Carlo approach, where several hundred simulations may sometimes be necessary.

Comparison of Monte Carlo and Rosenblueth Methods

In order to compare the Monte Carlo and Rosenblueth methods a series of IHDM simulations were carried out for all events. Tests were performed to determine the sensitivity of results to the number of Monte Carlo simulations, from which it was observed that little gain in accuracy was obtained using more than 500 realizations. In Figure 2 a comparison of the mean and 95% confidence limits (mean ±2 standard deviations) is made for the two methods, for event 1. The mean responses are virtually identical; however, for all events it was noted that the method of Rosenblueth tends to underestimate the variance of predictions. Nevertheless, considering the nonlinearity of the response function and that, for this study, Monte Carlo simulation requires over 30 times more computational effort, the results suggest that Rosenblueth's method serves as an efficient initial indicator of the magnitude of uncertainty.

Validity of Uncertainty Estimation

The nonlinear nature of the simulated hydrological responses also gives rise to a problem of representation of
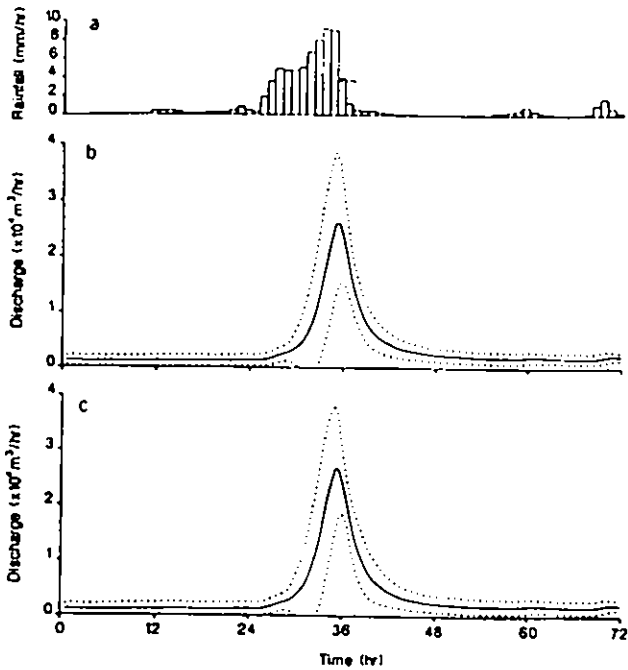
Fig. 2. (a) Hourly rainfall distribution for storm 1. (b) Predictive uncertainty using Monte Carlo simulation. (c) Predictive uncertainty using Rosenblueth's method. Solid line indicates mean flow, dashed lines indicate mean ±2 standard deviations.
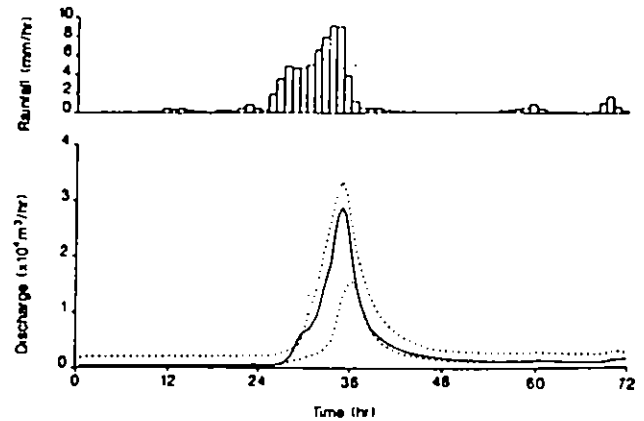

Fig. 3. Predictive uncertainty for storm 1 using Monte Carlo simulation. Solid line indicates observed flow, dashed lines indicate 5% and 95% simulation limits.

predictive uncertainty for both methods. The Rosenblueth method estimates, for every time step, a mean and variance for the predicted responses. The Monte Carlo simulations can be analyzed to yield the same information. The uncertainties shown in Figure 2 are based on these estimates. There is an implicit assumption in such an analysis that the distribution of the uncertain responses is normal at all time steps. The Monte Carlo simulations suggest that the assumption of normality is not justified for these simulations. One result of this is that the calculated lower 95% confidence limit (−2 standard deviations) will often be negative. To avoid this problem, the range of predictions in the remainder of this section have been calculated based on the rejection of the upper and lower 5% of the simulations, rather than using variance estimation which assumes knowledge of the distribution of responses.

Figures 3 and 4 show the predicted range and observed responses calculated on this basis for events 1 and 3, respectively. As events 1–5 are treated as calibration events one would hope that the predictive range of outflows envelopes the observed hydrograph. This, however, was not seen to be true throughout the entire simulation period for the two storms considered (events 1 and 3).

It should perhaps be pointed out at this stage that it is recognized that the observed flow is also associated with some degree of uncertainty. The measurement error for the Gwy flows is unknown, but may be of the order of 5–10% for all but the most extreme flow conditions. Pragmatism dictates that we accept the quality-checked flow data for the catchment as the best available estimate.

The time variability of the distribution of catchment outflows computed by the Monte Carlo simulations is shown in Figure 5 for event 3. At the time of peak of the mean flow the distribution is highly skewed, whereas at the end of the

simulation the distribution is reasonably symmetrical. The skewness is thought to reflect a tendency toward a maximum predictable runoff intensity for a particular rainstorm. Similar behavior was observed for all events considered and serves to support the use of 5 and 95 percentile limits as described above.

Storms 6 and 7 were considered as validation events and were within the range of magnitudes of the calibration events. Figures 6 and 7 show the 5% and 95% limits of the Monte Carlo simulations for events 6 and 7, respectively, together with the observed hydrographs. For both events the observed responses lie within the uncertainty envelope for a great proportion of the simulation period, the magnitude of any discrepancies being minimal. It is interesting to note, however, the position of the observed hydrograph relative to the uncertainty bounds for event 6. On the recession limb the observed response is similar to the lower uncertainty bounds, whereas during the rising limbs of the hydrograph the upper uncertainty limits are more characteristic of the observed flow. Similar behavior can be seen for the calibration events 1 and 3 in Figures 3 and 4, respectively, and reinforces the need for incorporating a predictive uncer-
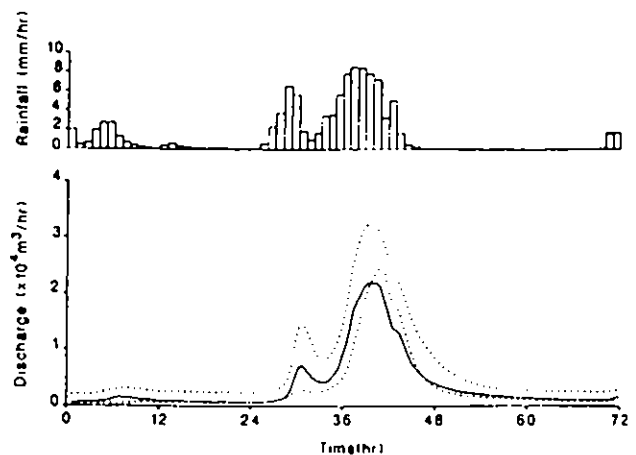

Fig. 4. Predictive uncertainty for storm 3 using Monte Carlo simulation. Solid line indicates observed flow, dashed lines indicate 5% and 95% simulation limits.
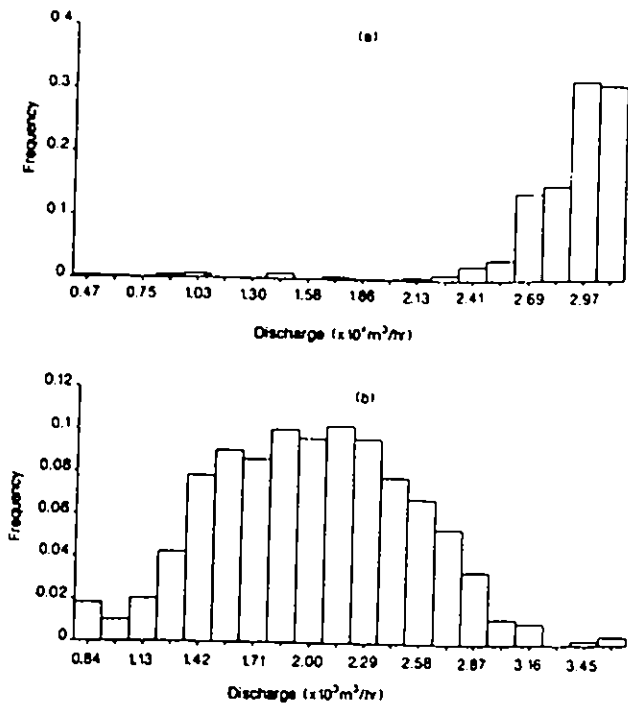
22

Fig. 7. Predictive uncertainty for storm 7 using Monte Carlo simulation. Solid line indicates observed flow, dashed lines indicate 5% and 95% simulation limits.

Fig. 5. Frequency distribution of predicted outflow rates for event 3 (a) at time of peak mean flow rate and (b) at end of simulation period.

later recession periods and closer to the upper limit during the wetting period.

EFFECT OF LAND USE CHANGE ON PREDICTIVE UNCERTAINTY

tainty framework within any physically based modeling methodology.

As can be seen from Table 1, storm 8 has a considerably higher peak flow than the events used for the calibration sequence and thus provides a more stringent validation test than the hydrographs of storms 6 and 7. Although measurements of catchment outflow are not available for the entire period of storm 8, the data obtained describe the main period of interest inadequately, including the peak flow rate. Figure 8 shows the position of the observed hydrograph in relation to the predictive uncertainty bounds. The observed flow rates compare favorably with the predictive range, particularly in respect of the limited number of the calibrated sequence of events. As noted earlier, the observed outflow tends to be closer to the lower uncertainty bound during the
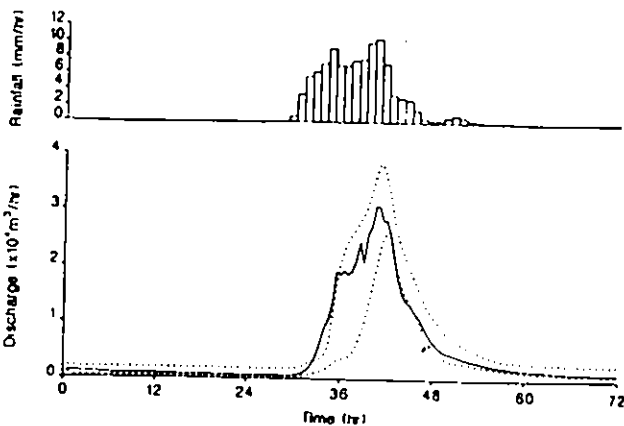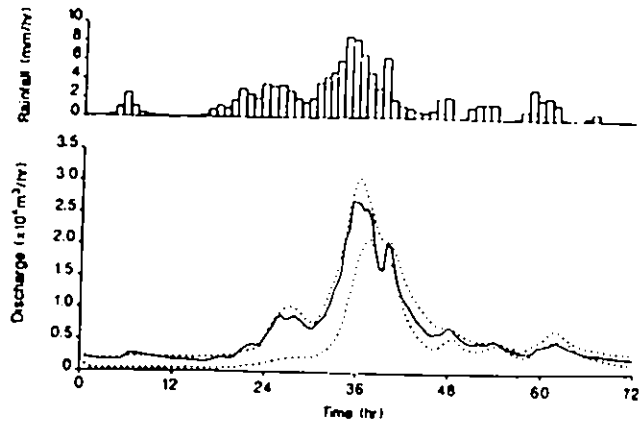
The Gwy catchment experiment is part of a long-term study carried out by the Institute of Hydrology into the effects of afforestation and deforestation on hydrological responses [see Calder and Newson, 1979]. Here, we address the problem of attempting to predict the effect of afforestation on the grassland Gwy catchment. Many catchment characteristics change as a result of afforestation, particularly where the planting of trees is associated with artificial drainage and road building, as is common in upland Britain. It is difficult to assess the effect of such changes on the parameters of a physically based model a priori, but it should be expected that the uncertainty bounds associated with the predictions should increase, relative to predictions for a calibrated catchment. The question that then arises is whether the predicted effects of land use change are statistically significant, within the limits of predictive uncertainty.

The sensitivity of uncertainty in predictions from the IHDM to land use characteristics was investigated by per-

Fig. 6. Predictive uncertainty for storm 6 using Monte Carlo simulation. Solid line indicates observed flow, dashed lines indicate 5% and 95% simulation limits.
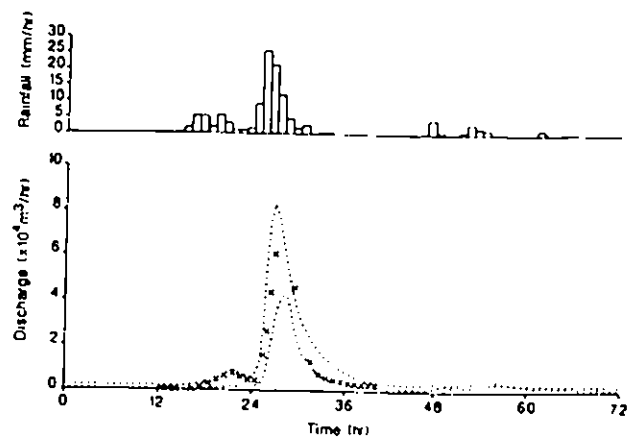
Fig. 8. Predictive uncertainty for storm 8 using Monte Carlo simulation. Crosses indicate observed flow, dashed lines indicate 5% and 95% simulation limits.
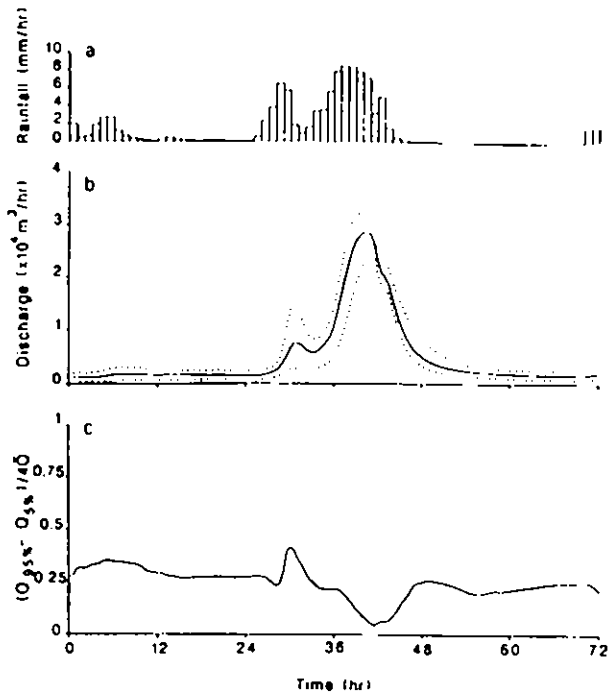
Fig. 9. Predictive uncertainty for storm 3 on grassland catchment. (a) Hourly rainfall distribution data. (b) Mean flow (solid line) and 5% and 95% limits (dashed lines). (c) Ninety percent limits expressed relative to mean flow.
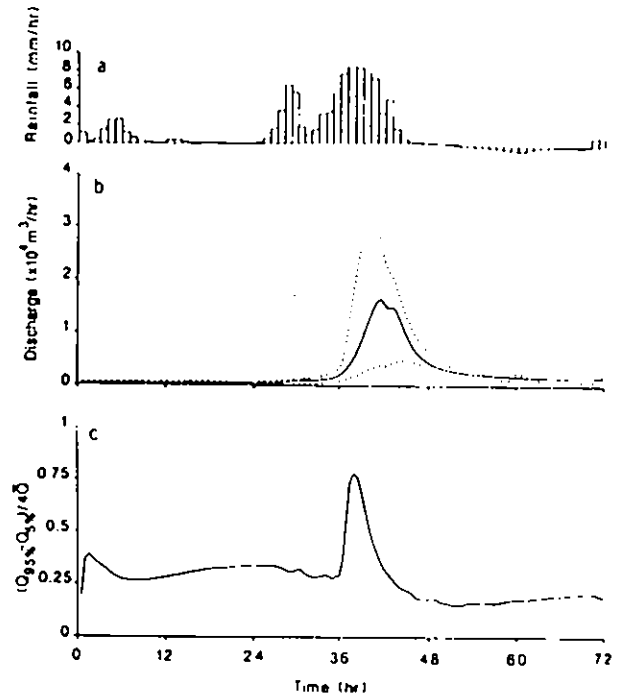

Fig. 10. Predictive uncertainty for storm 3 on forested catchment. (a) Hourly rainfall distribution data. (b) Mean flow (solid line) and 5% and 95% percent limits (dashed lines). (c) Ninety percent limits expressed relative to mean flow.

forming Monte Carlo simulations of storms 1 and 3 using the same parameter ranges as in Table 3, as before, but by adopting different parameter values for the preprogram of the IHDM (Table 2). The parameter values used are representative of forested catchments, rather than grassland catchments such as the Gwy. The forest parameters had been found to model net precipitation as measured at Plynlimon satisfactorily [Watts, 1988]. No uncertainty in these parameters was taken into account. Thus, we are making minimal changes to the model for the case of the forested catchment, but feel that this is justified on the grounds that a similar procedure would be followed in the case of a deterministic study of land use change without a priori knowledge of how soil parameters might change, that modeling studies of forested subcatchments of the River Severn at Plynlimon have led to soil and overland flow parameters within the ranges used here [Morris, 1980; Calver, 1988], and that we will be estimating minimum uncertainty bounds for the forested case. The initial condition parameter ψ_{in}, however, is likely at times to be significantly different for the forest and grassland catchments in that a more negative value (that is, drier conditions) is likely to result in the forested case from higher evapotranspiration losses and, in the case of reafforestation, possible artificial drainage channels. Based on soil water observations by Hudson [1988] a difference in matrix potential between forested and grassland catchments of 0.2 m water was considered reasonable. In order to accommodate such a difference the mean value of ψ_{in} was shifted by 0.2 m, together with the parameter minimum and maximum settings, keeping the variance constant.

Multiple simulations of the forested catchment were carried out for storms 1 and 3. Figures 9 and 10 show the mean and 90% confidence limits together with the time depen-

dence of the 90% limit relative to the mean flow for both grassland and forested cases for storm 3. The mean flow is clearly sensitive to the change in catchment characteristic. For example, a 42% reduction in mean peak flow was observed for event 3, in changing from grass to forested catchment. The difference in the predictions of peak flows can be tested statistically. In that the peak flows cannot be assumed to be normally distributed (Figure 5a) a nonparametric test should be used. Calculation of the Mann Whitney U statistic for the peak flow distributions of Figures 9 and 10 suggests that the difference in the median peak flow between forested and grassland catchments is highly significant (<0.001). The uncertainty limits also appear to be sensitive to the change, in particular at the peak flow. Again using storm 3 as an example, a 412% increase in the 90% limits relative to the mean flow, at the peak flow, resulted from grass to forest catchment predictions, although it should be noted that the main difference occurs during the peak of the event. It is interesting to note that little difference in mean and range of flows was observed when a similar Monte Carlo analysis was performed on land use change but maintaining the original (grassland) distribution for ψ_{in}. That is, the mean and uncertainty in predicted flows are apparently not sensitive to the parameters of the IHDM's preprogram without a change in initial conditions.

DISCUSSION

In a previous review of the use of physically based models in hydrology, Beven [1989] advocated that the predictions of such models must be associated with estimates of predictive uncertainty. This study has been in many ways a feasibility study and exploration of the techniques for uncertainty

estimation and their use in evaluating the predictions of such models. It is clear that we are still limited by the computational requirements of such models, both in parameter calibration and Monte Carlo uncertainty calculations. However, as computers become faster and cheaper, the Monte Carlo method may become more competitive as an operational technique. It is also well suited to use with parallel processing computing systems which will allow tens (or even hundreds) of runs of the model for the Monte Carlo uncertainty analysis to be made concurrently. The Monte Carlo simulations presented here were performed on the 80-node transputer-based Meiko computing surface at Lancaster University.

The results of this study suggest that we should expect the uncertainty bounds for physically based models to be quite wide, even when parameter values have been constrained by calibration. It has been shown that the Rosenblueth method allows a reasonable first estimation of the uncertainty limits on the basis of a small number of simulation runs, but the Monte Carlo method may be preferable if details of the distribution of responses are required, in particular where that distribution may be expected to be highly skewed.

The study of the effects of land use change reported above raises a number of interesting questions. It has been shown that, for the prediction of storm responses alone, changes in the predicted hydrographs resulting from changes in land use are, for the case of this catchment, large. However, this sensitivity is mainly due to changes in the initial conditions likely to result after land use change. The results, therefore, emphasize the importance of suitable parameter estimates and ranges if one is to predict the effect of changing catchment characteristics.

An interesting problem arising from this is, How can the uncertainties associated with both the calibration period and the predictions following change be constrained? Two strategies can be distinguished. For the case of the model calibration, it may be possible to constrain the estimated uncertainty ranges by incorporating more observed data into the calibration procedure. A longer period of observed discharges, observations of parameter values, and observations of internal state variables (such as water table levels) may all be useful in constraining uncertainty. An important point to note in this respect, however, is that it may be difficult to make use of parameter and internal state measurements that are of a very different scale from the grid scale of the model. How far the estimated uncertainties could be constrained in the Gwy predictions, given that they already do not always encompass the observed discharges for either calibration or validation storms, would make an interesting further study.

The present study does not negate certain advantages of the IHDM in providing a deterministic framework to assess the direction and relative magnitude of changes in hydrological response resulting from physical catchment changes. It is certain that in many cases, the magnitude of such changes will be greater than those investigated here and may prove significant in relation to uncertainty bounds. It is worth emphasizing, however, that in many cases it will be difficult to assess the effect of a land use change on the appropriate model predictions, and that such predictions should always be accompanied by a proper study of the associated uncertainties. Our aim here has been to outline a procedure by

which this might be achieved and look at the implications for one particular case study.

We would suggest that, in predicting the effects of land use change a priori, a realistic estimate of uncertainty will generally be high. It will only be possible to constrain those uncertainties by comparing the model predictions with observations as the change takes place. In this way forward predictions of change may become gradually more reliable. This argues for a continuing conjunctive use of modeling and field measurement where significant land use changes are being considered.

REFERENCES

Bathurst, J. C., Physically based distributed modelling of an upland catchment using the système hydrologique européen, *J. Hydrol.*, *87*, 79–102, 1986.

Beven, K. J., Changing ideas in hydrology: The case of physically based models, *J. Hydrol.*, *105*, 157–172, 1989.

Beven, K. J., and P. E. O'Connell, Physically-based models in hydrology, *Rep. 81*, Inst. of Hydrol., Wallingford, Oxon, England, 1982.

Beven, K. J., A. Calver, and E. M. Morris, The Institute of Hydrology distributed model, *Rep. 98*, Inst. of Hydrol., Wallingford, Oxon, England, 1987.

Calder, I. R., A model of transpiration and interception loss from a spruce forest in Plynlimon, central Wales, *J. Hydrol.*, *33*, 247–265, 1977.

Calder, I. R., and M. D. Newson, Land-use and upland water resources in Britain—A strategic look, *Water Resour. Bull.*, *15*, 1628–1639, 1979.

Calver, A., Calibration, sensitivity and validation of a physically-based rainfall-runoff model, *J. Hydrol.*, *103*, 103–115, 1988.

Calver, A., and W. L. Wood, On the discretisation and cost-effectiveness of a finite element solution for subsurface flow, *J. Hydrol.*, *110*, 165–179, 1989.

Freeze, R. A., and R. L. Harlan, Blueprint for a physically-based digitally-simulated hydrologic response model, *J. Hydrol.*, *9*, 237–258, 1969.

Guymon, G. L., M. E. Harr, R. L. Berg, and T. V. Hromadka II, A probabilistic-deterministic analysis of one-dimensional ice segregation in a freezing soil column, *Cold Reg. Sci. Technol.*, *5*, 127–140, 1981.

Hudson, J. A., The contribution of soil moisture storage to the water balances of upland forested and grassland catchments, *Hydrol. Sci. J.*, *33*(3), 289–309, 1988.

Monteith, J. L., Evaporation and environment, *Symp. Soc. Exp. Bot.*, *19*, 205–234, 1965.

Morris, E. M., Forecasting flood flows in grassy and forested basins using a deterministic distributed mathematical model, *Hydrological Forecasting, IASH Publ.*, *129*, 247–255, 1980.

Natural Environment Research Council, *Flood Studies Report*, 5 vols, London, 1975.

Newson, M. D., The Plynlimon floods of August 5–6th 1973, *Rep. 26*, Inst. of Hydrol., Wallingford, Oxon, England, 1975.

Rogers, C. C. M., K. J. Beven, E. M. Morris, and M. G. Anderson, Sensitivity analysis, calibration and predictive uncertainty of the Institute of Hydrology distributed model, *J. Hydrol.*, *81*, 179–191, 1985.

Rosenblueth, E., Point estimates for probability moments, *Proc. Natl. Acad. Sci. U. S. A.*, *72*(10), 3812–3814, 1975.

Rutter, A. J., and A. J. Morton, A predictive model of rainfall interception in forests, III, Sensitivity of the model to stand parameters and meteorological variables, *J. Appl. Ecol.*, *14*, 567–588, 1977.

Rutter, A. J., K. A. Kershaw, P. C. Robins, and A. J. Morton, A predictive model of rainfall interception in forests, I, Derivation of

the model from observations in a plantation of Corsican pine. *Agric. Meteorol.*, 9, 367–384, 1971.

Stephenson, G. R., and R. A. Freeze, Mathematical simulation of subsurface flow contributions to snowmelt runoff, *Reynolds Creek watershed, Idaho, Water Resour. Res.*, 10, 284–294, 1974.

Watts, L. G., The preprograms to the Institute of Hydrology distributed model, *Rep. 103*, 26 pp., Inst. of Hydrol., Wallingford, Oxon, England, 1988.

K. J. Beven and A. M. Binley, Centre for Research on Environmental Systems, Institute of Environmental and Biological Sciences, University of Lancaster, Lancaster LA1 4YQ, England.

A. Calver and L. G. Watts, Institute of Hydrology, Wallingford, Oxon OX10 8BB, England.

26

Dimensionless hillslope hydrology

A. CALVER, BSc, PhD, MIWEM*

W. L. WOOD, MA, PhD†

Slope discharge and its controlling variables are defined in a non-dimensional setting using the Buckingham π theorem. The method is general, although in this case data are drawn from numerical modelling of linked surface and subsurface flow equations, covering variably saturated throughflow and both infiltration-excess and saturation-excess overland flow. Nomographs are presented which can be used in a straightforward manner for discharge prediction or for parameter optimization. Two field examples are described in these contexts.

Notation

A	cross-sectional area of overland flow
b	exponent in overland flow rating curve
D	depth of permeable hillslope material
f	surface roughness coefficient
L	horizontal length of hillslope
k	hydraulic conductivity of slope material
k_s	value of k at saturation
Q	discharge per unit width of hillslope
Q_b	hillslope baseflow discharge per unit width
Q_p	peak value of hillslope discharge per unit width
r	rainfall rate
s	slope
t	time
t_p	time to peak discharge from beginning of rainfall
t_r	duration of rainfall
w	width of hillslope
θ	volumetric water content of slope material
θ_s	saturated value of θ, i.e. porosity
$\pi_1, \ldots, \pi_7$	dimensionless parameters of Buckingham theorem
ψ	pressure potential
ψ_{in}	initial value of ψ

Introduction

There is often a requirement for the simple and systematic presentation of hydrological data, whether observed or modelled, for purposes of rapid estimation. This may be considered particularly to be the case when the data are derived from complex models dealing with many parameters and using relatively long computer processing times. The expression of a hydrological problem, or indeed many other physical phenomena, in non-dimensional terms allows some degree of reduction in

parameter numbers and, importantly, facilitates the concise presentation of information on comprehensive ranges of situations.

2. The basic methodology of this Paper is specific neither to the physical situation nor to the method of deriving data. It is developed, however, in the context of discharge from hillslopes and small catchments for individual rainfall events, with data derived from numerical solutions of linked surface and subsurface flow equations. A major advantage of such modelling is its physical basis; one of its drawbacks, which the Authors aim to alleviate here, is the complexity of its use.

3. The methodology of the establishment of the relevant non-dimensional parameters is described, together with the derivation of modelled data. General results are presented to demonstrate a concise and comprehensive format, and two particular field examples are discussed to demonstrate the types of use of this approach in hydrological practice.

Methodology

Establishment of non-dimensional parameters

4. It is supposed that there is a dimensionally homogeneous (and hence unit free) physical law giving the discharge per unit width Q at the bottom of the hillslope in terms of the time t, the duration of the rainfall t_r, the rate of rainfall r (this is taken as the effective precipitation, after evaporation and interception), the saturated hydraulic conductivity k_s, the length L and depth D of the subsurface region, the initial value ψ_{in} of the pressure potential ψ throughout the region, the slope s, the porosity θ_s and the surface roughness f. It is also supposed that there is a free seepage face at the bottom of the slope, and the parameters which determine the non-linear variation of k/k_s and θ/θ_s with respect to ψ in the unsaturated zone are left fixed in this paper.

5. The Buckingham Pi theorem[1,4] states that this physical law is equivalent to an equation expressed only in dimensionless quantities. All the physical quantities involved can be expressed in the basic dimensions of length l and time t: t has dimension t, t_r has t, r has lt^{-1}, k_s has lt^{-1}, L has l, $-\psi_{in}$ has l, Q has l^2t^{-1}, and f has $l^{2\mu-b}t^{-1}$ (from the relationship of $Q = fs^{1/2}A^b$, where A is the cross-sectional area of the overland flow). Disregarding b, s and θ_s, which are already dimensionless, leaves the nine quantities Q, t, t_r, r, k_s, L, D, ψ_{in} and f which are functions of length and time.

6. In general, for n quantities which are functions of m dimensions, a set of $(n-m)$ independent dimensionless quantities can be found in terms of which the physical law can be expressed. Hence, in this problem, there are seven such dimensionless quantities. Similar considerations are, of course, employed in the design of scaled models (see, for example, Yalin[5]).

7. There are many ways of choosing these dimensionless quantities but they must be independent, in the sense of no functional relationship between the π parameters themselves. Using the Buckingham Pi notation, $\pi_1, \pi_2, \dots$ for the dimensionless parameters, it seems natural to take $\pi_1 = t/t_r$ (to relate the two times), $\pi_2 = L/D$ (to scale the subsurface regions), $\pi_3 = -\psi_{in}/D$ (keeping the parameters always positive; it also seems natural to link $-\psi_{in}$ with the depth rather than the length). After some experiment, the most convenient choice for the other parameters has been taken as $\pi_4 = Q/rL$ (relating the discharge to the rate at which water arrives on the whole length of slope), $\pi_5 = rt_r/L$ (the amount of rain per unit length of slope), $\pi_6 = r/k_s$ (another ratio of two like quantities as recom-

594

mended by Buckingham) and $\pi_7 = f^2 t_r/r$ (the surface roughness is here taken to be given by the Chézy formula, so that $b = 3/4$, and this parameter relates the surface roughness to the duration and intensity of the rainfall).

8. By the Buckingham Pi theorem, the dimensionless equation can be written in the form

$$\pi_4 = \frac{Q}{rL} = G(\pi_1, \pi_2, \pi_3, \pi_5, \pi_6, \pi_7) \tag{1}$$

On the right-hand side, π_1 is the only parameter involving the time t. Differentiating with respect to time, gives

$$\frac{1}{rL} \dot{Q} = \frac{\partial G}{\partial \pi_1} \frac{d\pi_1}{dt} = \frac{1}{t_r} \frac{\partial G}{\partial \pi_1} \tag{2}$$

The peak discharge is when $\dot{Q} = 0$: i.e. when $\partial G/\partial \pi_1 = 0$, and $t = t_p$, the time of the peak discharge. But this is equivalent to another dimensionless statement of the form

$$t_p/t_r = F(\pi_2, \pi_3, \pi_5, \pi_6, \pi_7) \tag{3}$$

Equation (1) also gives

$$Q_p/rL - G(t_p/t_r, \pi_2, \pi_3, \pi_5, \pi_6, \pi_7) \tag{4}$$

where Q_p is the peak discharge.

9. Hence, substituting from equation (3) in equation (4) gives an equation of the form

$$Q_p/rL = H(\pi_2, \pi_3, \pi_5, \pi_6, \pi_7) \tag{5}$$

The formulae given by equations (3) and (5) are used as the basis for the numerical results. Each computer simulation is given a run-in time before the start of the rainfall. After this time, the baseflow Q_b is changing only very slowly, and the rise in flow $(Q_p - Q_b)$ is taken as the significant flow to plot. The figures presenting the results are described in §§ 15–22.

10. There appears to have been little specific reference to the Buckingham Pi theorem in hydrological methodology: exceptions are the papers of Wong[6] and Gowda and Lock[7], but these are not relevant to the problem in hand. Woolhiser and Liggett[8] set the Saint Venant equations in non-dimensional forms for the rising surface flow hydrograph, and this approach is extended by Morris and Woolhiser[9] Many hydrological papers make use of a partially, rather than a completely, non-dimensional setting. Skempton et al.[10] for example, propose the ratio of the 'storm response' change in groundwater level to the total quantity of rainfall as a characteristic parameter for a site, and Oakes and Wilkinson[11] using modelled data, address the problem of natural and pumped regimes in the saturated zone, using dimensionless groupings to reduce parameter numbers.

Derivation of modelled data

11. Subsurface hillslope flow, of variably saturated nature, is modelled using Darcy's Law and mass conservation considerations, and is solved by a two-dimensional Galerkin finite-element method. Surface runoff on hillslopes, whether derived from infiltration excess or from saturation excess, is modelled by a one-dimensional kinematic wave formulation, solved by a four-point finite difference

595

29

scheme. These features are combined in the Institute of Hydrology Distributed Model, and further details are available in, for example, Beven et al.,[12] Calver and Wood,[13] and Wood and Calver;[14] reference to particular details will be made later in this Paper.

12. It is self-evident that, in expressing results of runoff simulations in terms of non-dimensional parameter groupings, a single result may be achieved from a variety of combinations of physical parameters. As the modelling requires numerical rather than analytical solution because of the complexity of conditions, it is important to check the discretization of the problem in its effect on the degree of scatter of results achieved from different but non-dimensionally similar parameter groupings. Aspects of the discretization into quadrilateral elements used in the subsurface part of the model have been investigated previously (Calver and Wood[13]). For the establishment of discharge estimation curves for interpolation, it is considered necessary, in order to avoid the scatter, to use the comparatively high cpu (central processing unit) times of vertical to horizontal element size ratio of 1:1 and a length of 0·5 m. In a number of contexts, an element aspect ratio of up to 1:20 may be appropriate, but it can lead to differences in results depending on the
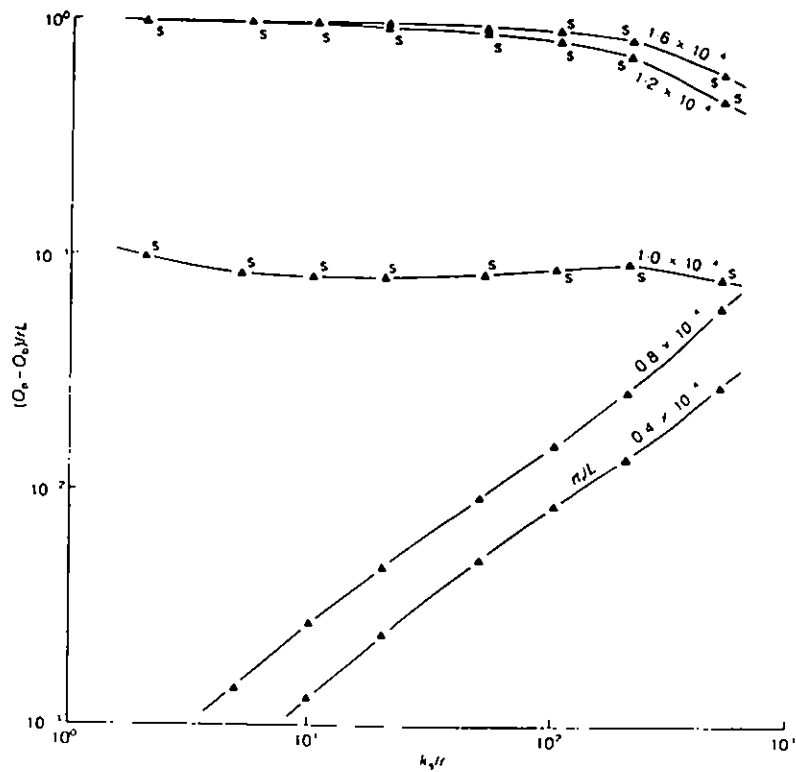

Fig. 1. Peak discharges and causal variables. For parameter details, see text; spatially constant initial condition. The letter s beside a data point indicates that discharge includes saturation-excess overland flow in addition to subsurface flow

596

30

parameter grouping used. Calver and Wood[13] note that 80% of discharge results using a 1:20 ratio were within ±10% of the 1:1 discretization results. These considerations are of particular importance when the threshold to overland flow production is likely to be crossed.

13. It is a matter of choice which parameter set is employed in obtaining a result. In the present work, r is held constant at (5 mm h^{-1}), and t, and k, are varied. The numerical tests above in the context of discretization confirm this does not greatly affect results. However, it is important to note that there are practical limits on the numerical ranges of parameter values. For example, some combinations of rainfall intensity and duration are more appropriate physically than others (see, for example, the *Flood studies report*, vols 2 and 5,[15] for the UK case; Institution of Engineers[16] for Australia, etc.). In the simulations undertaken here, t, is varied between 4 and 16 hours, and k, between 0·025 and 2·5 m h^{-1}.

14. The model is run on a Cray X-MP on which typical cpu times for simulation of one event are in the order of 3–5 min. The run-in time of 100 modelled hours before the introduction of rainfall allowed the establishment of numerical stability and only very slowly varying hydrological conditions.

Dimensionless presentation of results

15. Figures 1–4 demonstrate the presentation of hillslope discharge results for a 500 m 1-in-10 slope, with 1·5 m of permeable material of porosity 0·4 and surface Chézy roughness of 20 000 m$^{0·5}$ h^{-1}. The relationships of unsaturated hydraulic conductivity and water content to pressure potential are assumed to be single value functions representative of a medium textured soil.[17] Saturated throughflow discharge occurs from a seepage face above channel water level. Two commonly considered initial conditions are used. In Figs 1 and 2, pressure potential in the
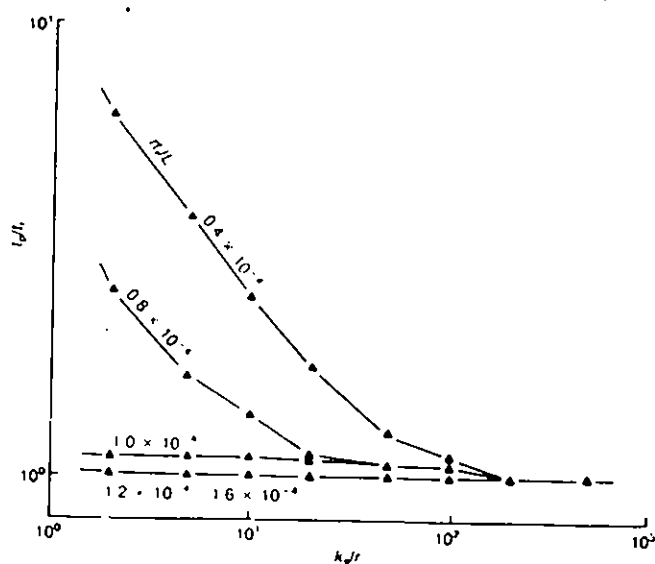

Fig. 2. Time-to-peak and causal variables. For parameter details, see text; spatially constant initial condition

hillslope material is everywhere set at a constant value, here -0.3 m. In practice, using a run-in period, this is a convenient way of establishing a drainage profile of slightly wetter conditions lower in the soil profile by the time rainfall is introduced. In Figs 3 and 4, an elevation-related initial condition is specified such that the soil is wetter not only in the lower part of a soil profile, but also lower on the slope: i.e. further from the drainage divide. Specifically in this example, pressure potential at a point is set at one-tenth of the elevation difference between that point and the foot of the slope. The form of the figures is explained below, with reference to the processes operative in the modelling.

16. Figures 1 and 3 deal with peak discharges; Figs 2 and 4 with the time of its occurrence. The horizontal axis in all cases denotes the ratio of saturated hydraulic conductivity (lt^{-1}), a measure of travel rate, to the rate of water addition to the slope (lt^{-1}). The vertical axes in Figs 1 and 3 denote the ratio of peak discharge above baseflow per unit width (l^2t^{-1}) to the rainfall input to unit width of slope (l^2t^{-1}). The vertical axes in Figs 2 and 4 show the ratio of time-to-peak to duration of rainfall. Individual curves are drawn for rt_r/L values, i.e., total depth of rainfall
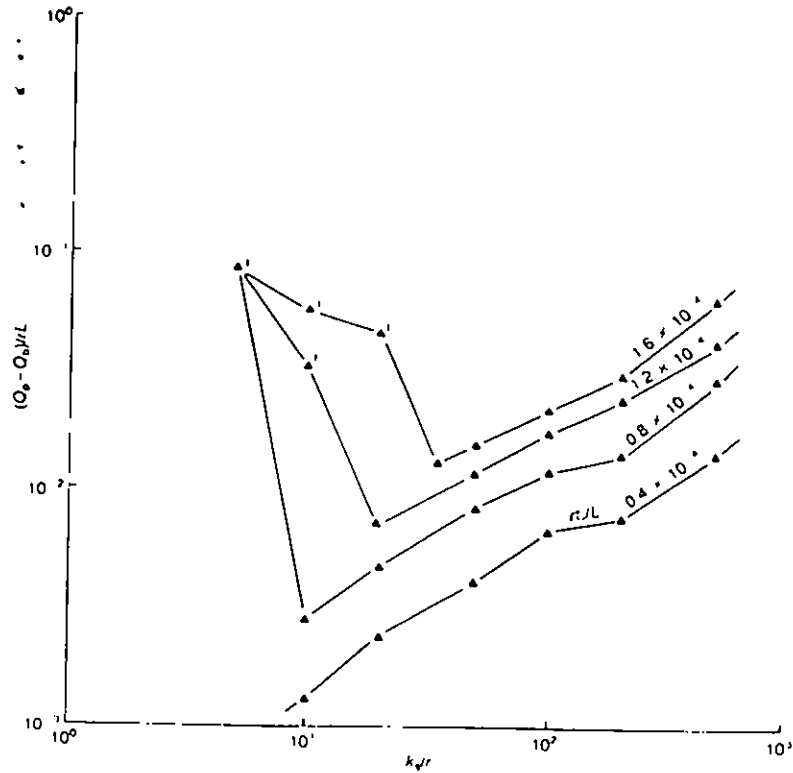

Fig. 3. Peak discharges and causal variables: elevation-related initial condition. The letter i beside a data point indicates that runoff includes infiltration-excess overland flow in addition to subsurface flow

598

32

as a ratio of slope length. The indiviual segments of these curves are drawn as straight lines between the calculated points.

17. In Fig. 1, all discharge responses involve saturated throughflow discharge at the foot of the slope. The three uppermost rt_e/L curves also involve overland flow derived, in these cases, from the upward over-saturation of the soil profile over part of the slope and the subsequent surface routing of that excess water. Problems including overland flow show higher $(Q_p - Q_b)/rL$ values, in cases approaching unity. For lower k_s/r and higher rt_e/L values there is an increased likelihood of build-up of soil saturation promoting saturation-excess overland flow. As k_s/r increases, higher throughflow discharge occurs.

18. Fig. 2 shows the corresponding times-to-peak of the Fig. 1 peak discharges. A decline in time-to-peak is seen towards that of the time of the end of the (constant intensity) rainfall as k_s/r increases. This minimum time is reached at lower k_s/r for the higher rt_e/L cases, i.e. those promoting some fast surface flow.

19. Figures 3 and 4 follow the same principles but for the elevation-related initial condition. The right-hand part of the diagram reflects throughflow discharge increasing with k_s/r in a generally similar manner to Fig. 1, but without the production of saturation-excess overland flow. This is due to higher subsurface conductivities associated with the wetter conditions in the lower part of the slope.
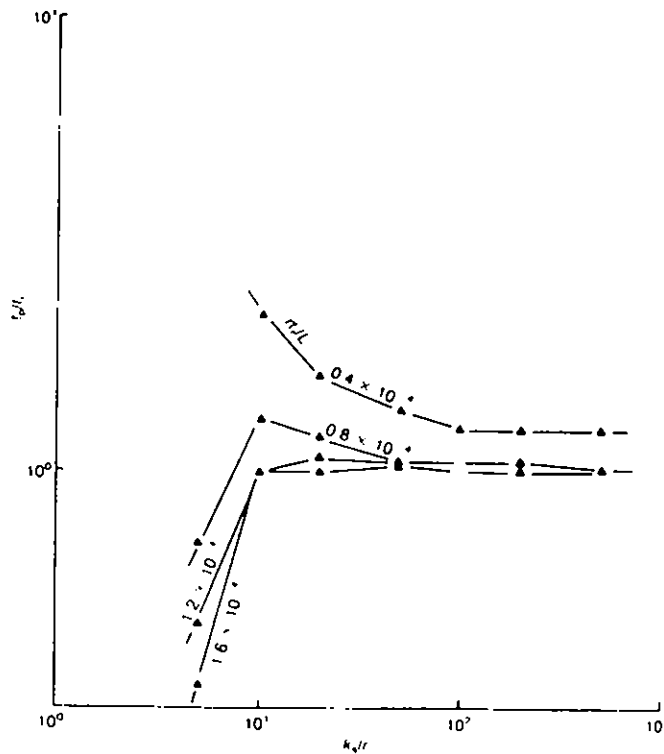

Fig. 4 Times-to-peak and causal variables: elevation-related initial condition

599

However, the upper part of the slope, by definition, is considerably drier than that of Fig. 1, to the extent that, in some cases, the prevailing low conductivities reduce infiltration capacity to the degree that infiltration-excess overland flow is produced, for the lower k_s/r values, promoting greater $(Q_p - Q_b)/rL$ values. These, however, do not approach the contributing areas or discharges of the saturation-excess overland flow of Fig. 1.

20. These discharge processes are reflected in Fig. 4 where the features of Fig. 2 are seen, together with some t_p/t_r values < 1 for the low k_s/r values which indicate the production of infiltration-excess overland flow early in the storm event and the domination of peak discharge by this flow rather than by the later throughflow response.

21. The significance of the overland flow/throughflow division lies not only in the magnitude and timing of discharge: it also has important implications for the chemistry of water entering the stream system and for the potential for surface erosion.

22. Figures 1–4 illustrate the Authors' methology and the range of processes covered. In the following, the detail of two field examples is considered and the different types of use are demonstrated.

Types of use

Field examples

23. The first example is taken from an Institute of Hydrology experimental catchment in central Wales, the 0.9 km² Tanllwyth catchment. Runoff occurs by way of surface and subsurface flow. In the modelling an approximation for average slope width is required, the slope in this case being one encircling both sides and the top of the stream channel. This is a convenient approximation for a small catchment which has been tested before. The storm of 12 February 1976 is used as an example event on this catchment, approximated by constant intensity rainfall relevant to that producing a peak flow: i.e. not including the tail of the storm. The measured rainfall and runoff for this event are given in Calver [18] who also describes runoff modelling in the catchment. The data for the catchment and for this storm are as follows: $r = 0.00435$ m h⁻¹, $t_r = 12$ h, $w = 2100$ m, $L = 800$ m, $D = 1.5$ m, $wQ_b = 0.05$ m³ s⁻¹, $k_s/r = 230$, $\psi_{in} = -0.1$ m.

24. A plot in the format of Figs 1 and 3, namely of $(Q_p - Q_b)/rL$ against k_s/r, can be used in a number of ways. If, for example, it is assumed that all physical parameters are known (or have been obtained by optimization), the plot can be used to give peak flow above baseflow for any storm. For the 12 February 1976, event $(Q_p - Q_b)/rL$ is interpolated as 0.71 and hence wQ_p is estimated at 1.49 m³ s⁻¹; the observed peak for the catchment is 1.71 m³ s⁻¹.

25. The second field example is that of discharge from a hillslope with pseudo-gley soils developed on Keuper Marl near Larochette, Luxembourg. (This area is a site of field measurements and modelling of runoff generation by the Institute of Hydrology and the University of Amsterdam.) Here there are three distinct soil horizons of different material properties, the uppermost of which, the AEh horizon, is known to have varying hydraulic conductivity over time, between approximately 0.2 and 1.8 m h⁻¹, resulting from annual cycles of physical and biological processes. The slope and event data are as follows: $r = 0.002$ m h⁻¹; $t_r = 5$ h; $w = 40$ m; $L = 100$ m; $D(\text{total}) = 0.36$ m; $D(\text{AEh horizon}) = 0.09$ m; $wQ_p = 1.2 \times 10^{-3}$ m s⁻¹(gauged), $Q_b = 0$ (i.e. flow is intermittent), $\psi_{in}(\text{AEh horizon}) = -1.3$ m, $\psi_{in}(\text{elsewhere}) = $ depth below AEh horizon.

600

26. Using a $(Q_p - Q_b)/rL$ against k_s/r plot, for known parameter values except the AEh conductivity, for the measured runoff event of 20 October 1988, an effective k_s value of this event of 0.4 m h^{-1} is derived.

General use

27. It will be apparent, therefore, that, if the numerical values of physical variables relevant to a problem are known, the types of dimensionless nomograph derived here can be used for the quick estimation of event runoff, either for a particular event of interest or for a design storm.

28. It is frequently the case that discharge has been measured but uncertainty exists over the value of a particular parameter; hydraulic conductivity is a common example. The nomographs can be used to determine the operative value of the parameter. Confidence is increased by the convergence on a particular numerical value of a constant parameter from the separate consideration of a number of events.

29. This parameter optimization procedure occurs commonly at the earlier stages of model fitting, before predictive mode use. The Plynlimon example of predictive use (above) had previously undergone optimization of a number of parameter values.[18]

30. The detail of presentation of discharge results by the general method given here may be tailored to specific needs. For example, if porosity variability is an important element, this can be included as a variable rather than as a constant; similarly with surface roughness. If further detail of the rainfall distribution is considered important, a two-parameter triangular or normal distribution can be incorporated. For the purposes of the analyses described here, it is considered important to have a minimum of two parameters for rainfall description.

Conclusions

31. This Paper has demonstrated the expression of slope discharge results in relation to causal variables in a concise and non-dimensional manner based on the Buckingham π theorem. The hydrological processes covered are saturated and unsaturated throughflow, and overland flow caused by infiltration-excess and/or saturation-excess.

32. This demonstration has used modelled data from numerical solutions of standard surface and subsurface flow equations. The method is, however, appropriate to, and may prove useful for, data derived from other sources, whether measured or modelled.

33. The type of nomographs derived can be used for estimation in a straight-forward manner in both parameter-optimazation mode and discharge-prediction mode, as illustrated by the field examples described.

Acknowledgement

References

1 BUCKINGHAM E. On physically similar systems: illustrations of the use of dimensional equations *Physical Review*, 1914, 4, 345-376.
2 BUCKINGHAM E. Model experiments and the forms of empirical equations. *Trans Am. Soc. Mech. Engrs*, 1915, 37, 263-296

3. Birkhoff G. *Hydrodynamics: a study in logic, fact and similitude*. Princeton University Press, Princeton, NJ, 1960.

4. Lixian J. D. *Applied mathematics: a contemporary approach*. Wiley, Chichester, 1987.

5. Yalin M. S. *Theory of hydraulic models*. Macmillan, London, 1971.

6. Wong S. T. A dimensionally homogeneous and statistically optimal model for predicting mean annual flood. *J. Hydrol.*, 1979, 42, 269–279.

7. Gowda T. P. H. and Lock J. D. Volatilization of organic chemicals of public health concern. *J. Environ. Enqng Div. Am. Soc. Civ Enqrs*, 1985, 111, 755–776.

8. Woolhiser D. A. and Liggett J. A. Unsteady, one-dimensional flow over a plane—the rising hydrograph. *Water Resources Res.* 1967, 3, 753–771.

9. Morris E. M. and Woolshiser D. A. Unsteady one-dimensional flow over a plane: partial equilibrium and recession hydrographs. *Water Resources Res.* 1980, 16, 355–360.

10. Skempton A. W. *et al.* The Mam Tor Landslide, North Derbyshire. *Phil. Trans. R. Soc.*, 1989, 329, 503–547.

11. Oakes D. B. and Wilkinson W. B. *Modelling of groundwater and surface water systems. 1: theoretical relationships between groundwater abstraction and base flow.* Water Resources Board, Reading, 1972, Publication 16.

12. Beven K. *et al. The Institute of Hydrology distributed model.* Institute of Hydrology, Wallingford, 1987, Report 98.

13. Calver A. and Wood W. L. On the discretization and cost-effectiveness of a finite-element solution for hillslope subsurface flow. *J. Hydrol.*, 1989, 110, 165–179.

14. Wood W. L. and Calver A. Lumped versus distributed mass matrices in the finite element solution of subsurface flow. *Water Resources Res.*, 1990, 26, 819–825.

15. Natural Environment Research Council. *Flood studies report.* NERC, 1975, 2 and 5.

16. The Institution of Engineers, Australia. *Australian rainfall and runoff. A guide to flood estimation.* Institution of Engineers, Barton ACT, 1987.

17. Clapp R. B. and Hornberger G. M. Empirical equations for some soil hydraulic properties. *Water Resources Res.*, 1978, 14, 601–604.

18. Calver A. Calibration, sensitivity and validation of a physically-based rainfall-runoff model. *J. Hydrol.*, 1988, 103, 103–115.

602

IHDM PUBLICATIONS

Beven, K, Calver, A and Morris, E (1987), The Institute of
    Hydrology Distributed Model. Institute of Hydrology Report
    No. 98.

Calver, A (1988), Calibration, sensitivity and validation of a
    physically-based rainfall-runoff model. Journal of Hydrology,
    103,103-115.

Watts, L.G. (1988), The Preprograms to the Institute of
    Hydrology Distributed Model. Institute of Hydrology Report
    No. 103.

Calver, A. and Wood, W.L. (1989), On the discretisation and cost-
    effectiveness of a finite element solution for hillslope
    subsurface flow. Journal of Hydrology, 110, 165-179.

Wood, W.L. and Calver, A. (1990), Lumped versus distributed mass
    matrices in the finite element solution of subsurface flow.
    Water Resources Research, 26, 819-825.

Calver, A. and Binning, P. (1990), On hillslope water flow paths
    and travel times. Journal of Hydrology, 121, 333-342.

Roberts, G., Calver, A. and France, M. (1990), The use of remote
    sensing and geographic information systems for providing the
    parameter requirements of the Institute of Hydrology
    Distributed Model. Presented European Geophysical Conference,
    Copenhagen.

Watts, L.G. and Calver, A. (1991), Effects of spatially-
    distributed rainfall on runoff using a physically-based model.
    Nordic Hydrology, 22, 1-14.

Calver, A and Wood, W.L. (1991), Dimensionless hillslope
    hydrology. Proceedings of the Institution of Civil
    Engineers,   part 2, 91, 593-602.

Binley, A.M., Beven, K.J., Calver, A. and Watts, L.G. (1991),
    Changing responses in hydrology: assessing the uncertainty in
    physically-based model predictions. Water Resources Research,
    27, 1253-1261.

Wood, W.L. and Calver, A. (in press), Initial conditions for
    hillslope hydrology modelling. Journal of Hydrology.

Institute of
Hydrology

Natural
Environment
Research
Council